Supplemental material to this article can be found at:
http://jpet.aspetjournals.org/content/suppl/2018/11/09/jpet.118.251413.DC1

1521-0103/368/2/157–168$35.00
THE JOURNAL OF PHARMACOLOGY AND EXPERIMENTAL THERAPEUTICS
https://doi.org/10.1124/jpet.118.251413
J Pharmacol Exp Ther 368:157–168, February 2019
Copyright © 2019 The Author(s).
This is an open access article distributed under the CC BY Attribution 4.0 International license.

The Journal of PHARMACOLOGY And Experimental Therapeutics

Towards Further Verification of Physiologically-Based Kidney Models: Predictability of the Effects of Urine-Flow and Urine-pH on Renal Clearance[S]

Takanobu Matsuzaki,[1] Daniel Scotcher,[1] Adam S. Darwich, Aleksandra Galetin, and Amin Rostami-Hodjegan

Centre for Applied Pharmacokinetic Research, University of Manchester, Manchester, United Kingdom (T.M., D.S., A.S.D., A.G., A.R.-H.); Research Laboratories for Development, Shionogi & Co., Ltd., Osaka, Japan (T.M.); and Simcyp Limited (A Certara Company), Sheffield, United Kingdom (A.R.-H.)

Received June 28, 2018; accepted November 5, 2018

ABSTRACT

In vitro-in vivo extrapolation (IVIVE) of renal excretory clearance (CL_R) using the physiologically based kidney models can provide mechanistic insight into the interplay of multiple processes occurring in the renal tubule; however, the ability of these models to capture quantitatively the impact of perturbed conditions (e.g., urine flow, urine pH changes) on CL_R has not been fully evaluated. In this work, we aimed to assess the predictability of the effect of urine flow and urine pH on CL_R and tubular drug concentrations (selected examples). Passive diffusion clearance across the nephron tubule membrane was scaled from in vitro human epithelial cell line Caco-2 permeability data by nephron tubular surface area to predict the fraction reabsorbed and the CL_R of caffeine, chloramphenicol, creatinine, dextroamphetamine, nicotine, sulfamethoxazole, and theophylline. CL_R values predicted using mechanistic kidney model at a urinary pH of 6.2 and 7.4 resulted in prediction bias of 2.87- and 3.62-fold, respectively. Model simulations captured urine flow–dependent CL_R, albeit with minor underprediction of the observed magnitude of change. The relationship between drug solubility, urine flow, and urine pH, illustrated in simulated intratubular concentrations of acyclovir and sulfamethoxazole, agreed with clinical data on tubular precipitation and crystal-induced acute kidney injury. This study represents the first systematic evaluation of the ability of the mechanistic kidney model to capture the impact of urine flow and urine pH on CL_R and drug tubular concentrations with the aim of facilitating refinement of IVIVE-based mechanistic prediction of renal excretion.

Introduction

Together with the liver, the kidneys play a principal role in the excretion of a wide variety of xenobiotics, including drugs, metabolites, and toxins, as well as endogenous compounds. Renal excretion can be defined as the elimination of unchanged solutes from the blood into the urine as a net result of the processes of glomerular filtration, tubular secretion, and tubular reabsorption (Tucker, 1981).

Passive tubular reabsorption is a major process that controls the extent of renal excretion of many substances (Varma et al., 2009; Scotcher et al., 2016b). The magnitude of passive reabsorption depends on the lipophilicity and extent of ionization of a drug and physiologic properties, such as urine flow rate and the pH of the luminal fluid in the renal tubule (Tang-Liu et al., 1983). Urine flow and urine pH-dependent CL_R have been reported for several drugs (Beckett et al., 1969; Sharpstone, 1969; Tang-Liu et al., 1982; Blanchard and Sawers, 1983; Birkett and Miners, 1991). Such trends are often mechanistically rationalized by the Henderson-Hasselbalch equation as arising from perturbed tubular reabsorption (Tucker, 1981; Molander et al., 2001).

In addition, urine flow and urine pH can be important contributors to renal toxicity risk. Sulfamethoxazole and acyclovir are low-solubility compounds, and crystalluria leading to acute kidney injury (AKI) reported for these drugs has been attributed to changes in urine flow and urine pH (Perazella, 1999). Direct measurement of the concentration of drugs in renal tubules compared with compound solubility properties may be beneficial in managing such risk. In the absence of direct measurements of intratubular concentrations in humans, use of mechanistic models representing pharmacokinetic processes within the proximal tubules in a physiologically meaningful context may provide useful insights and inferences in a quantitative manner.

[1]T.M. and D.S. equally contributed to this work.

T.M. is an employee of Shionogi & Co., Ltd. D.S. was supported by a Ph.D. studentship from the Biotechnology and Biological Sciences Research Council UK [BB/J500379/1] and AstraZeneca. A.R.-H. is an employee of Simcyp Limited (A Certara Company).
https://doi.org/10.1124/jpet.118.251413.
[S] This article has supplemental material available at jpet.aspetjournals.org.

ABBREVIATIONS: AAFE, absolute average fold error; AFE, average fold error; AKI, acute kidney injury; $CL_{int,efflux}$, intrinsic efflux clearance; $CL_{int,HLM}$, intrinsic metabolic clearance in human liver microsome; $CL_{int,uptake}$, intrinsic uptake clearance; $CL_{PD,x}$, passive permeability clearance across membrane x; CL_R, renal excretion clearance; DT, distal tubule; IVIVE, in vitro to in vivo extrapolation; LoH, loop of Henle; MATE, multidrug and toxin extrusion protein; MCD, medullary collecting ducts; MechKiM, mechanistic kidney model; OAT, organic anion transporters; P_{app}, apparent permeability; PBPK, physiologically based pharmacokinetics; PT, proximal tubule; V_{ss}, volume of distribution at steady state.

Downloaded from jpet.aspetjournals.org at ASPET Journals on March 13, 2024

To predict human renal excretion clearance (CL_R), an in vitro-in vivo extrapolation (IVIVE)–based approach using a mechanistic renal tubular reabsorption model was previously reported and validated with a set of 45 drugs that undergo limited secretion (Scotcher et al., 2016b). Advantages of this model include separation of drug- and physiologic/system-specific information, which allows potential extrapolation to populations with different pathophysiologic features. Despite its physiologic nature, an important limitation of this static model was that urine flow–dependent CL_R could not be adequately described, which also limits simulation of intratubular drug concentrations.

Theoretically, mechanistic kidney models developed within a physiologically based pharmacokinetic (PBPK) modeling framework can resolve the preceding limitations; however, these models typically include a large number of parameters, and measured data to inform some of the system (physiologic) parameters may not exist (e.g., proximal tubule cellularity) or are associated with uncertainty (e.g., renal transporter abundances) (Neuhoff et al., 2013; Scotcher et al., 2016a). In addition, some parameters may exhibit biologic variability that is not controlled or monitored in a typical clinical study; for example, urinary pH can range from 4.5 to 8, but it is generally slightly acidic (i.e., 5.5–7.0) because of metabolic activity (Simerville et al., 2005). Another challenge with such complex models is ensuring the identifiability of parameters as plasma concentration-time data may not always be informative for all model parameters (Hsu et al., 2014; Huang and Isoherranen, 2018), as discussed previously (Tsamandouras et al., 2015; Scotcher et al., 2017; Guo et al., 2018). All the preceding challenges are also applicable in the case of renal elimination, especially when attempting to separate quantitatively the roles of active transport and passive permeability to overall secretion and/or reabsorption (e.g., salicylic acid, creatinine). Therefore, independent verification of specific model assumptions relating to passive permeability of drugs in the kidney would be of benefit since this is currently lacking.

The overall aim of this study was to assess the accuracy of a mechanistic kidney model for simulation of CL_R and intratubular concentrations under perturbed conditions, particularly changes in urine flow and urine pH, when only effects relating to passive permeability were considered. Mechanistic description of active processes was not addressed; readers interested in this topic are directed elsewhere (Hsu et al., 2014; Posada et al., 2015; Ball et al., 2017). The accuracy of IVIVE-based predictions of both CL_R and fold changes in CL_R from urine flow or pH changes was evaluated for caffeine, chloramphenicol, creatinine, dextroamphetamine, nicotine, sulfamethoxazole, and theophylline. Criteria for their selection included the availability of clinical data under perturbed conditions for CL_R, particularly changes in urine flow and urine pH. Subsequently, the ability of the kidney model to simulate intratubular concentrations was investigated for low-solubility drugs acyclovir and sulfamethoxazole. The effects of variations in urine flow and urine pH were assessed to evaluate the likelihood of precipitation risk associated with crystalluria. Clinical reports on the effect of urine flow or pH changes on the occurrence of crystalluria for these two drugs were used for indirect validation of the simulated intratubular drug concentrations. Implications of the findings on the mechanistic prediction of tubular reabsorption and CL_R using IVIVE-PBPK modeling are discussed.

Materials and Methods

Development of Initial PBPK Model without Mechanistic Kidney Model. A literature search in PubMed identified seven drugs for which CL_R and urine flow rates were simultaneously reported in the same subjects; these drugs were caffeine, chloramphenicol, creatinine, dextroamphetamine, nicotine, sulfamethoxazole, and theophylline. In addition, acyclovir and sulfamethoxazole were selected to assess the relationship between tubular concentrations and solubility owing to their association with crystalluria. Mean plasma concentration-time profiles and pharmacokinetic parameters were collated from the reported clinical studies (Table 1). Pharmacokinetic parameters of interest were the area under the curve for the plasma concentration-time profile, the intravenous clearance and apparent oral clearance, volume of distribution at steady state (V_{ss}) and CL_R. Where necessary, data were digitized using WebPlotDigitizer (versions 3.12 and 4.0, https://automeris.io/WebPlotDigitizer). Where necessary, CL_R values were calculated from the urinary excretion rate (urine concentration × urine flow rate) divided by its plasma concentration or total urine excretion amount divided by the area under the curve.

All simulations presented herein were performed using the Simcyp simulator, version 16, release 1 (Certara, Sheffield, UK) (Jamei et al., 2009, 2013). Drug-dependent parameters for the initial PBPK models without implementation of the MechKiM are listed in Supplemental Tables S1 and S2. All simulations were performed using the default "healthy volunteers" population template file in the Simcyp simulator. The workflow used for the refinement and verification of compound files in the full PBPK model, as required for use of MechKiM, is shown in Fig. 1.

For the whole-body PBPK models, distribution parameters—including V_{ss} and tissue-to-plasma partition coefficients (Kp)—were predicted using the modified Rodgers and Rowland method (Rodgers et al., 2005; Rodgers and Rowland, 2006; Gaohua et al., 2016). Predicted Kp values were optimized by an empirical scalar (same factor used for all tissues) to recover the observed V_{ss}, as estimated from observed plasma-concentration profiles using parameter estimation module in the simulator (weighted least-squares fitting, weighted by the reciprocal of the predicted value squared). No refinement of predicted Kp was necessary for creatinine (Kp scalar = 1). Metabolic clearance and CL_R input parameters for the caffeine and theophylline PBPK models were not changed from the default values. The intrinsic hepatic metabolic clearance parameters (for amphetamine, chloramphenicol, and nicotine were obtained using back-calculation of CL_{int} from available intravenous clearance data using the well stirred model and correcting for CL_R.

After verification of the clearance and distribution parameters, first-order oral absorption model parameters, fraction absorbed (F_a), and the absorption rate constant (k_a) were optimized and verified for caffeine, creatinine, dextroamphetamine, and theophylline. Since the production rate of creatinine is reported to be 18.72 mg/kg per day in human (Boroujerdi, 1982), an i.v. infusion dosing of 18.72 mg/kg per day was implemented to mimic the production rate of creatinine. The cooked-meat meal is suggested to contain about 340 mg of creatinine (Mayersohn et al., 1983); therefore, oral administration of 340 mg of creatinine was assumed for this condition. Data used for verification were from independent clinical studies different from those used for parameter refinement and developing the model; details of clinical studies collated are listed in Table 1. During verification and refinement of PBPK models, simulations in 10 trials of virtual subjects were performed after trial designs (dosing route, amount, and frequency; number of individuals; and age of subjects) reported in the respective publications.

Prediction of Tubular Reabsorption in MechKiM: Physiologic Parameters and Scaling Approach. Previously reported IVIVE-based static tubular reabsorption model (Scotcher et al., 2016b) is a five-compartment mechanistic model comprising segments representing the glomerulus proximal tubule (PT), the loop of Henle (LoH), the distal tubule (DT), and the collecting ducts (CD) (Scotcher et al., 2016b). In contrast, MechKiM comprises eight segments

Downloaded from jpet.aspetjournals.org at ASPET Journals on March 13, 2024

TABLE 1
Details of clinical studies used for verification and refinement of the physiologically based pharmacokinetics models for selected compounds

Compound	Reference	Optimization/Verification	Dose Information	Subject Information
Caffeine	Lelo et al. (1986)	Refinement	270-mg oral SD	6 M, 19–21 yr
	Newton et al. (1981)	Verification	50-mg oral SD	5 M, 21–36 yr
	Newton et al. (1981)	Verification	300-mg oral SD	5 M, 1 F, 21–36 yr
	Newton et al. (1981)	Verification	500-mg oral SD	5 M, 1 F, 21–36 yr
	Newton et al. (1981)	Verification	750-mg oral SD	5 M, 1 F, 21–36 yr
Chloramphenicol	Burke et al. (1982)	Refinement	CAPS 502– to 1324-mg i.v. infusion for average of 18 min SD	3 M, 5 F, 19–64 yr
	Mikami et al. (1975)	Verification	1000-mg i.v. SD, bolus (1 min)	15 M, 40–53 yr
	Nahata and Powell (1981)	Verification	CAPS 100-mg/kg per day i.v. infusion over 0.5 h	1 M, 20 yr
Creatinine	Mayersohn et al. (1983)	Verification	Baseline	6 M, 26–38 yr
	Mayersohn et al. (1983)	Verification	Cooked meat (340-mg oral)	6 M, 26–38 yr
Dextroamphetamine	Watanalumlerd et al. (2007)	Refinement	20- or 30-mg oral	Not reported
	Beckett et al. (1969)	Refinement	8.7-mg oral SD	2 M, 21 and 23 yr
	Dolder et al. (2017)	Verification	29.6-mg oral SD	12 M, 12 F, 21–34 yr
	Wan et al. (1978)	Verification	10-mg oral SD	4 M, 1 F, 22–26 yr
Nicotine	Molander et al. (2001)	Refinement	0.028-mg/kg i.v. infusion for 10 min SD	10 M, 10 F, 22–43 yr
	Benowitz and Jacob (1993)	Refinement	0.015-mg/kg i.v. infusion for 30 min SD	9 M, 2 F, 22–58 yr
	Zevin et al. (1997)	Verification	0.015-mg/kg i.v. infusion for 30 min SD	6 M, 6 F, 18–47 yr
Sulfamethoxazole	Mannisto et al. (1982)	Refinement	1000-mg i.v. infusion for 60 min SD	4 M, 2 F, 22–31 yr
	Welling et al. (1973)	Refinement	800-mg oral SD	6 subjects
	Welling et al. (1973)	Refinement	800-mg oral SD	5 subjects
	Hutabarat et al. (1991)	Verification	10-mg/kg i.v. infusion for 60 min SD	7 M, 1 F, 22–27 yr
	Kaplan et al. (1973)	Verification	2000-mg oral SD	24 M
	Kaplan et al. (1973)	Verification	2000-mg oral SD	8 M
Theophylline	Lelo et al. (1986)	Refinement	250-mg oral SD	6 M, 19–21 y
	Rovei et al. (1982)	Verification	125-mg oral SD	4 M, 4 F, 22–35 yr
	Rovei et al. (1982)	Verification	250-mg oral SD	4 M, 4 F, 22–35 yr
	Rovei et al. (1982)	Verification	375-mg oral SD	4 M, 4 F, 22–35 yr
	Rovei et al. (1982)	Verification	500-mg oral SD	4 M, 4 F, 22–35 yr
Acyclovir	Blum et al. (1982)	Refinement	0.5- to 15-mg/kg, 1- or 6-h infusion	Not reported
	Soul-Lawton et al. (1995)	Refinement	350-mg, 1-h infusion	4 M, 8 F, 23–50 yr
	Brigden et al. (1981)	Verification	50-mg i.v. bolus SD	6 M, 26–38 yr
	Brigden et al. (1981)	Verification	50-mg i.v. 1 h infusion	2 M, 26–38 yr
	Brigden et al. (1981)	Verification	50-mg i.v. 10 min infusion	2 M, 26–38 yr
	de Miranda et al. (1981)	Verification	0.5- to 2.5-mg/kg, i.v. infusion over 1 h	1 M, 4 F, 25–68 yr
	Laskin et al. (1982a)	Verification	5-mg/kg i.v. infusion over 1 h	1 M, 2 F, 24–67 yr
	Laskin et al. (1982b)	Verification	2.5-mg/kg, i.v. infusion over 1 h	5 M, 8 F, 23–76 yr
	Laskin et al. (1982b)	Verification	5.0-mg/kg, i.v. infusion over 1 h	5 M, 8 F, 23–76 yr
	Laskin et al. (1982b)	Verification	10-mg/kg, i.v. infusion over 1 h	5 M, 8 F, 23–76 yr
	Laskin et al. (1982b)	Verification	15-mg/kg, i.v. infusion over 1 h	5 M, 8 F, 23–76 yr

CAPS, chloramphenicol succinate; F, female; M, male; SD, single dose.

representing the glomerulus, three subregions of PT (PT-1, PT-2, and PT-3), the LoH, the DT, and the cortical and medullary collecting ducts (MCDs) (Neuhoff et al., 2013). The MechKiM parameterizes passive permeability of drugs across the tubular epithelium as permeability clearances through the apical ($CL_{PD,\ apical}$) and basolateral ($CL_{PD,\ basal}$) membranes rather than a "drug-specific" apparent permeability (P_{app}) and a "system-specific" tubular surface area.

In this study, an IVIVE approach was adapted from the static model for prediction of passive tubular reabsorption (Scotcher et al., 2016b). P_{app} values across Caco-2 cell monolayers were obtained from various literature sources, and details for each individual drug investigated are listed in Supplemental Table S3. The passive permeability in MechKiM is applied to the unbound and un-ionized species. According to Henderson-Hasselbalch equations, chloramphenicol, dextroamphetamine, nicotine, and sulfamethoxazole are estimated to have a smaller fraction in un-ionized form at apical (donor side, pH 6.5) and basolateral side (receiver side, pH 7.4) in the pH gradient format of the Caco-2 permeability assay (Supplemental Fig. S1; Supplemental Table S4). In vitro P_{app} measurements across Caco-2 cell monolayers can be affected by the drug characteristics (e.g., lipophilicity, pKa, unbound fraction in buffer and cells, and unspecific adsorption to in vitro systems) and assay conditions (e.g., buffer pH, rotation speeds, transporters, and density of cell monolayer). Full details of the assay conditions were not consistently reported alongside the Caco-2 P_{app} data that were collected from the literature. Therefore, to calculate the CL_{PD} used in MechKiM, the assumption was made that literature reported Caco-2 P_{app} values were representative of the passive permeability of unbound and un-ionized drug.

The apparent membrane permeability was calculated on the basis that resistance is the inverse of permeability and by assuming that the membrane resistance associated with the Caco-2 cell monolayer is attributable to the sum of resistances associated with the apical and basolateral membranes (eq. 1) (Avdeef, 2012; Kramer, 2016). This method makes several assumptions: the permeability of drugs across the apical membrane is equal to that of the basolateral membrane; no significant accumulation or binding of drug within the cell; assay is performed under sink conditions and no relevant effects of the filter support, aqueous boundary layer or para-cellular pathway:

$$\frac{1}{P_{app}} = \frac{2}{P_{mem}} \quad (1)$$

The apparent membrane permeability was scaled to $CL_{PD,\ apical}$ and $CL_{PD,\ basal}$ using regional tubular surface area (TSA), as IVIVE scaling factor for each ith tubular section represented by the model (eq. 2):

$$CL_{PD,i} = P_{mem} \times TSA_i \quad (2)$$

Tubular surface areas for each tubular section were recalculated to adapt to MechKiM from the reported values for the five-compartment model (Supplemental Table S5) (Scotcher et al., 2016b) and are listed in Table 2. The CL_{PD} values for each drug are shown in Supplemental Table S6.

Downloaded from jpet.aspetjournals.org at ASPET Journals on March 13, 2024

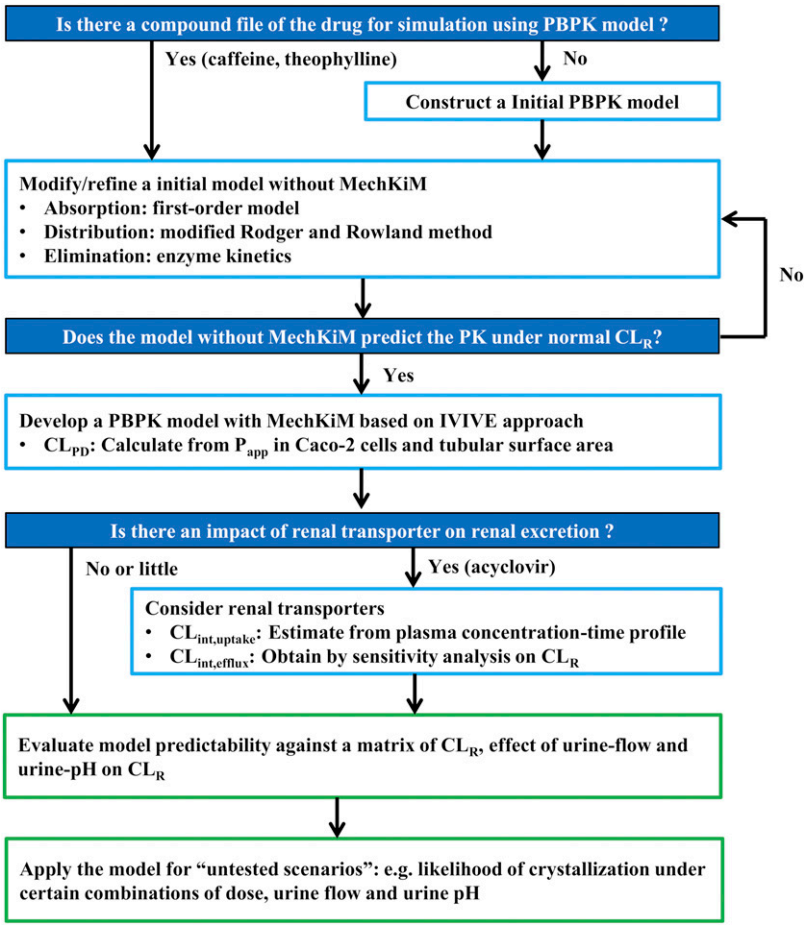

Fig. 1. Workflow of the development and qualification of the PBPK kidney model.

Predictive performance of the model against F_{reab} and CL_R parameters was assessed for several compounds. The focus of the work was on renal elimination and corresponding changes in CL_R; therefore, the predictive performance of plasma concentration-time profiles was not assessed. Transporter contribution was assumed to be negligible for the compounds investigated. Although in vitro data indicate involvement of renal transporters in some instances (e.g., creatinine), the roles of filtration and/or passive permeability to renal elimination are expected to be dominant. Simulations were performed according to the reported clinical study designs in 10 trials of virtual subjects from the healthy volunteer population provided in the software. The effect of different assumed values for urinary pH on prediction of CL_R was investigated by fixing the urine pH parameter to 7.4 (Simcyp default value) or 6.2 (Rose et al., 2015). Owing to the lack of measured data on segmental filtrate pH in humans (Neuhoff et al., 2013), tubular pH was assumed to be the same as urinary pH in this study. To compare the predictability of different models, the prediction of CL_R by the static model was also assessed, as described previously (Scotcher et al., 2016b). The tubular surface area and tubular flow rate values used for the static model are listed in Supplemental Table S7.

Development of PBPK Model for Acyclovir in MechKiM and Consideration of Active Secretion. Acyclovir is rapidly excreted in the urine via glomerular filtration and tubular secretion via renal transporters, including organic anion transporter (OAT)1, OAT2, OAT3, multidrug and toxin extrusion (MATE)1, and MATE2-K (Takeda et al., 2002; Tanihara et al., 2007; Ito et al., 2010; Cheng et al., 2012; Ye et al., 2012, 2013; Mathialagan et al., 2017). The predicted CL_R value of acyclovir in MechKiM without considering renal transporters (i.e., filtration clearance only) was 115 ml/min, thereby underpredicting the observed CL_R value of 283 ml/min (Soul-Lawton et al., 1995) (Supplemental Table S8). Accurate mechanistic representation of transporter kinetics for acyclovir was out of the scope of this study, and therefore an operational model was developed to simulate this compound's active secretion. The operational model, featuring a single basolateral transporter–mediated uptake clearance and a single apical efflux clearance, was developed using a previously described stepwise approach (Hsueh et al., 2018). First, a $CL_{int,\ uptake}$ value for uptake transport in the renal proximal tubules was determined by fitting the in vivo plasma concentration-time profile (Soul-Lawton et al., 1995) (weighted least-squares fitting, weighted by the reciprocal of the predicted value squared); a $CL_{int,\ efflux}$ value of 1 μl/min per million proximal tubule cells was fixed as a reference value (Hsueh et al., 2018). Second, using the resulting $CL_{int,\ uptake}$ value (14.0 μl/min per million proximal tubule cells), the $CL_{int,\ efflux}$ value (1.15 μl/min per million proximal tubule cells) was obtained by sensitivity analysis of the observed CL_R data (283 ml/min (Soul-Lawton et al., 1995)) (Supplemental Fig. S2). The simulated concentration-time profiles were in good agreement with observed data (Supplemental Fig. S3). Finally, observed acyclovir CL_R data reported by other clinical studies were used for model verification (Supplemental Table S8).

Simulation of Urine Flow–Dependent CL_R. Effects of variations of urine flow on CL_R were simulated for each drug using the virtual population representative (male, age 20 years, body weight 81 kg) in a healthy volunteer population. Dosage information used for simulations is listed in Supplemental Table S9. Urine and tubule pH values of 4.5, 6.2, and 8.0 were used to investigate the impact of the fraction of drug as un-ionized species. The relative change in CL_R was calculated using CL_R predicted when urine flow rate = 1 ml/min as baseline. Focus of the work was on relative changes as a result of perturbed renal elimination, analogous to approaches applied for

Downloaded from jpet.aspetjournals.org at ASPET Journals on March 13, 2024

TABLE 2

Tubular surface area used to calculate passive permeability clearance (CL_{PD}) in mechanistic kidney model

Values recalculated from those reported for the five-compartment model (Scotcher et al., 2016b).

	Tubular Surface Area (cm^2/million tubule cells)
PT-1	2.98
PT-2	2.98
PT-3	2.98
LoH	0.0796
DT	0.101
CCD	0.0184
MCD	0.00374

CCD, Cortical collecting duct; DT, distal tubule; LoH, loop of Henle; MCD, medullary collecting duct; PT, proximal tubule.

the evaluation of drug-drug or drug-disease interactions (e.g., (Yoshida et al., 2017). Changes in plasma drug concentrations from urine flow variations are typically small and not frequently reported and so were not evaluated in the current study. Baseline CL_R at urine flow rate of 1 ml/min was calculated from reported clinical data over a flow range; details for individual drugs and clinical studies are shown in Supplemental Table S10.

Tubular flow-rate input parameter values used in the MechKiM and the static model are listed in Supplemental Tables S11 and S12, respectively. To maintain mass balance, Simcyp MechKiM tubular outflow rates were matched to the inflow rates of the subsequent tubule compartment. Therefore, the inflow rate to the first proximal tubule compartment was defined as the glomerular filtration rate and was set to 120 ml/min. Bladder urine flow rates in MechKiM ranged from 0.1 to 20.0 ml/min to cover the range observed in clinical studies measuring CL_R; the adjusted flow-rate values were calculated by the Simcyp software for the remaining tubular compartments. In clinical observations, patients with reported acyclovir-induced AKI showed low urine output of approximately 0.1–0.2 ml/min (Giustina et al., 1988; Eck et al., 1991). Although higher urine flow rate values (up to approximately 28 ml/min) have been reported in humans under extreme water diuresis, clinical CL_R data under this condition were not found in literature (Supplemental Table S13).

In the case of the static tubular reabsorption model, midpoint flow rates were assumed for each tubular region; the highest flow rate investigated (11.6 ml/min) was determined by the assumed flow rate at the beginning of the collecting duct, and the urine flow rate range from 0.1 to 11.6 ml/min. The flow rates for the remaining tubular regions were not changed in the static model assuming that changes to urine flow rate are mediated by changes to water permeability in only the collecting duct. This assumption is in accordance with current understanding of the physiologic regulation of water balance via a feedback mechanism involving osmoreceptor, arginine vasopressin, and aquaporin (Knepper et al., 2015).

Simulation of Urine pH-Dependent CL_R. Effects of variations of urine pH on CL_R were simulated for each drug using a generic virtual study design of 10 trials of 10 subjects (proportion of females, 0.5; age, 20–50 years) in a healthy volunteer population. Dosage information for simulations is shown in Supplemental Table S9. The fluid pH at each tubule (PT, LoH, DT, and CD) varied from 4 to 9, assuming the same for urine pH. Glomerular filtration rate values for virtual subjects were calculated using the Cockcroft-Gault equation, based on serum creatinine, age, and weight of the defined virtual population, and bladder urine flow rates were 1 ml/min. Observed data obtained from the literature are listed in Supplemental Table S10. Data were presented graphically as fold changes in CL_R from baseline values at either 1 ml/min urine flow rate or pH 6.2. As with the urine flow simulations, primary focus was on the magnitude of changes rather than the absolute values.

Simulation of Tubular Concentration for Acyclovir and Sulfamethoxazole. Acyclovir and sulfamethoxazole are associated with the precipitation of crystals in the distal tubular lumen, including collecting ducts in patients and nonhuman animals (Brigden et al., 1982; Tucker, 1982; Tucker et al., 1983; Sawyer et al., 1988; Perazella, 1999). To evaluate the relationship between tubular concentration and solubility, tubular concentrations of acyclovir and sulfamethoxazole were simulated using the population representative (a 20-year-old man; body weight, 81 kg) in a healthy volunteer population. In addition, urine concentration was calculated from simulated excreted urine amount and urine flow rate by sampling at regular intervals for 0.25, 1, 3, or 6 hours. The solubility of acyclovir is 2.5 mg/ml in water at 37°C (Arnal et al., 2008), and sulfamethoxazole shows pH-dependent solubility (0.51 mg/ml at pH 4.11, 0.61 mg/ml at pH 5.48, 8.25 mg/ml at pH 7.16, 37.7 mg/ml at pH 7.79) in aqueous buffer at 37°C (Dahlan et al., 1987). Urine flow rate for simulation was fixed to 1 (control), 0.2 (assuming volume depletion), or 5 ml/min (assuming fluid therapy). Urine pH used for acyclovir simulation was set at the median value of pH 6.2, whereas a pH range between 4 and 8 was investigated for sulfamethoxazole due to urine pH sensitive CL_R.

Data Analysis. The predictability of the PBPK model and the other approaches was assessed by calculating the average fold error (AFE), the absolute average fold error (AAFE), and root mean square error, according to eq. 3–5:

$$AFE = 10^{\left(\frac{1}{n}\sum log\left(\frac{Predicted}{Observed}\right)\right)} \quad (3)$$

$$AAFE = 10^{\left(\frac{1}{n}\sum \left|log\left(\frac{Predicted}{Observed}\right)\right|\right)} \quad (4)$$

$$RMSE = \sqrt{\frac{1}{n}\sum \left(\log(Observed) - \log(Predicted)\right)^2}, \quad (5)$$

where n is the number of assessed studies for each drug. In addition, the percentage of studies within 2-fold and 3-fold was assessed by comparison of the predicted and observed pharmacokinetic parameters.

Results

PBPK Models without Mechanistic Kidney Model. Compound-specific input parameters for the developed PBPK models of the investigated drugs are listed in Supplemental Table S1 and S2. The simulated concentration-time profiles before activation of mechanistic kidney model were generally in good agreement with observed data for all drugs (Supplemental Fig. S4). Although some misspecification of the absorption phase may be apparent for some drugs (or could not be fully verified with available clinical data), accurate description of oral absorption was not considered an essential feature of the model for the purpose of the current study, and therefore further refinement of oral absorption was not performed.

Prediction of CL_R Using Mechanistic Kidney Model. Subsequently, CL_R was predicted using IVIVE of tubular reabsorption for seven drugs/endogenous molecules, namely, caffeine, chloramphenicol, creatinine, dextroamphetamine, nicotine, sulfamethoxazole, and theophylline. Predictions were performed using a mechanistic kidney model and following different urinary pH assumptions (Supplemental Fig. S5; Table 3). Urinary and tubular pH levels at average condition (i.e., without coadministration of ammonium chloride or sodium bicarbonate for urine acidification or alkalification, respectively) were assumed to be either 7.4 (Simcyp default value) or 6.2 (Rose et al., 2015). Overall predictability of CL_R using the MechKiM model was poorer compared with the static model, reflected in the AAFE of 3.62, 2.87, and 1.97

Downloaded from jpet.aspetjournals.org at ASPET Journals on March 13, 2024

TABLE 3

Prediction accuracy of renal clearance of seven drugs predicted using mechanistic kidney model (MechKiM) and mechanistic renal tubular reabsorption model (static model)

For simulation using MechKim, urine/tubular pH at average condition was used as 7.4 (Simcyp default value) and 6.2 (Rose et al., 2015). Details of predictions are listed Supplemental Material, Supplemental Table S14.

	AFE	AAFE	RMSE	% 2-fold	% 3-fold
MechKiM (pH 7.4)	3.39	3.62	29.1	26.3	57.9
MechKiM (pH 6.2)	2.69	2.87	37.9	52.6	68.4
Static model[a]	1.42	1.97	18.4	68.4	73.7

AAFE, absolute average fold error; AFE, average fold error; RMSE, root mean square error.

[a]Scotcher et al. (2016b).

for the MechKiM model at pH 7.4 and 6.2, and the static reabsorption model, respectively (Table 3). Use of urinary pH of 6.2 improved the predictability of CL_R using the mechanistic kidney model relative to pH 7.4; however, these differences typically arose from relatively small differences in predicted F_{reab} (Supplemental Table S15). Urinary pH had no impact on simulated CL_R for caffeine, creatinine, dextroamphetamine, and theophylline (Supplemental Fig. S5). Simulated CL_R at pH 6.2 was in better agreement with the observed data for chloramphenicol and sulfamethoxazole compared with pH 7.4, whereas opposite trends were seen for nicotine. Based on this analysis, pH 6.2 was used as baseline urine pH in MechKiM for subsequent simulations of the average condition.

As expected, simulation of acyclovir CL_R without consideration of renal transporters resulted in a substantial underprediction of CL_R (Supplemental Table S8). When renal transporters were accounted for using an operational model, simulated CL_R of acyclovir was in close agreement with observed values (predicted/observed ratio: 0.93), and no impact of pH was noted. The simulated concentration-time profiles using MechKiM at urine pH of 6.2 are shown in Fig. 2. The simulations of systemic profiles were generally in agreement with the model where prediction of CL_R was not done in a mechanistic manner.

Simulation of Urine Flow–Dependent CL_R. The impact of changes in urine flow rate on the simulated CL_R of eight selected drugs was assessed (see Fig. 3) by changing the relevant tubular flow rate parameters in the mechanistic kidney model while keeping urine pH constant at 4.5, 6.2, and 8.0. Overall, prediction of changes in CL_R at different urine flow rates by MechKiM showed better consistency with observed data than predictions using the static model. The model predictions identified caffeine, sulfamethoxazole, and theophylline as the compounds with the largest relative change in CL_R resulting from changes in urine flow rate, in agreement with observed data; however, an overall underprediction of the magnitude of urine flow–dependent changes in CL_R was apparent. This underprediction trend was particularly evident for sulfamethoxazole in the acidic urine condition. In the current data set, use of urinary pH 6.2 resulted in the best agreement with predicted change in CL_R for caffeine, creatinine, and theophylline. The simulated trend in CL_R for chloramphenicol at urinary pH 4.5 was generally in agreement with observed data. Although simulations for nicotine under acidic condition (pH 4.5) predicted a urine flow–dependent CL_R, the magnitude of this predicted effect was small. The large variability in the observed nicotine CL_R data and the small range of corresponding urine flow rates made it difficult to determine the true extent of covariability for this drug. No effects of urine flow on predicted CL_R of creatinine and acyclovir were seen; these are low-permeability compounds (P_{app} = 1.08 and 0.291 $\times$ 10^{-6} cm/s, respectively).

Simulation of Urine pH–Dependent CL_R. Simulated impact of changes in urine pH on the CL_R of the eight drugs was also assessed (Fig. 4) by changing the urine and tubular fluid pH in MechKiM while keeping the urine flow rate constant at 1 ml/min in 100 virtual healthy subjects. Simulated CL_R rates of chloramphenicol, nicotine, and sulfamethoxazole were sensitive to urine pH over the range of 4.5–8.0, whereas no effect was seen for remaining compounds. The trends in simulated pH-dependent changes in CL_R for sulfamethoxazole were largely in agreement with the observed data, although the observed trends for nicotine and dextroamphetamine were not recovered. In the cases of chloramphenicol, theophylline, and acyclovir, the accuracy of prediction could not be assessed because of a lack of clinical CL_R values reported with corresponding urine pH data.

Simulation of Renal Tubular Concentrations of Acyclovir and Sulfamethoxazole. High-dose acyclovir was reported to result in crystal-induced AKI (Sawyer et al., 1988; Perazella, 1999). A low dose of this drug is typically well tolerated but can also cause AKI in the presence of severe volume depletion (urine output: 350 ml/24 hours) (Giustina et al., 1988). Analogous to acyclovir, sulfamethoxazole can cause AKI in the presence of acidic urine (pH $<$ 7.15) (Perazella, 1999). Tubular concentrations of acyclovir and sulfamethoxazole were simulated by using doses for which crystal-induced AKI have been reported. Simulations of acyclovir PK and CL_R at high doses (500 mg/m^2 i,v. infusion, three times daily for 14 days) indicated that MCD was the tubular region with the highest C_{max} (Fig. 5A). The predicted acyclovir MCD tubular filtrate C_{max} was 4.69 mg/ml at normal urine flow rate (1 ml/min), which exceeds the reported aqueous solubility of 2.5 mg/ml. Urinary concentrations calculated from simulated data for urine sampling every 0.25 hour were comparable to the simulated MCD tubule concentrations, whereas urine sampling at 3-hour intervals or longer showed less agreement (Fig. 5B). At a low dose (5 mg/kg i.v. infusion, daily for 2 days) predicted concentrations of acyclovir in MCD tubule were below aqueous solubility at normal urine flow, but above aqueous solubility cut-off when urine flow was low (0.2 ml/min, Fig. 6A). Similarly, simulation of high dose (25 mg/kg four times daily for 14 days) of sulfamethoxazole with normal urine flow rate (1 ml/min) predicted C_{max} in MCD tubules equal to its solubility when pH $<$ 7 (Fig. 6B). In addition, low urine flow rate increased tubular concentration of sulfamethoxazole beyond its aqueous solubility limit. Simulation of high urine flow of 5 ml/min markedly decreased the C_{max} of acyclovir and sulfamethoxazole in MCD tubules; in this condition, their simulated tubular C_{max} levels were below the solubility limit.

Discussion

Several mechanistic pharmacokinetic kidney models have been reported in the literature, with some recent efforts focusing predominantly on describing in vivo roles of transporter kinetics without mechanistically accounting for passive permeability (Felmlee et al., 2013; Neuhoff et al., 2013; Dave

Downloaded from jpet.aspetjournals.org at ASPET Journals on March 13, 2024

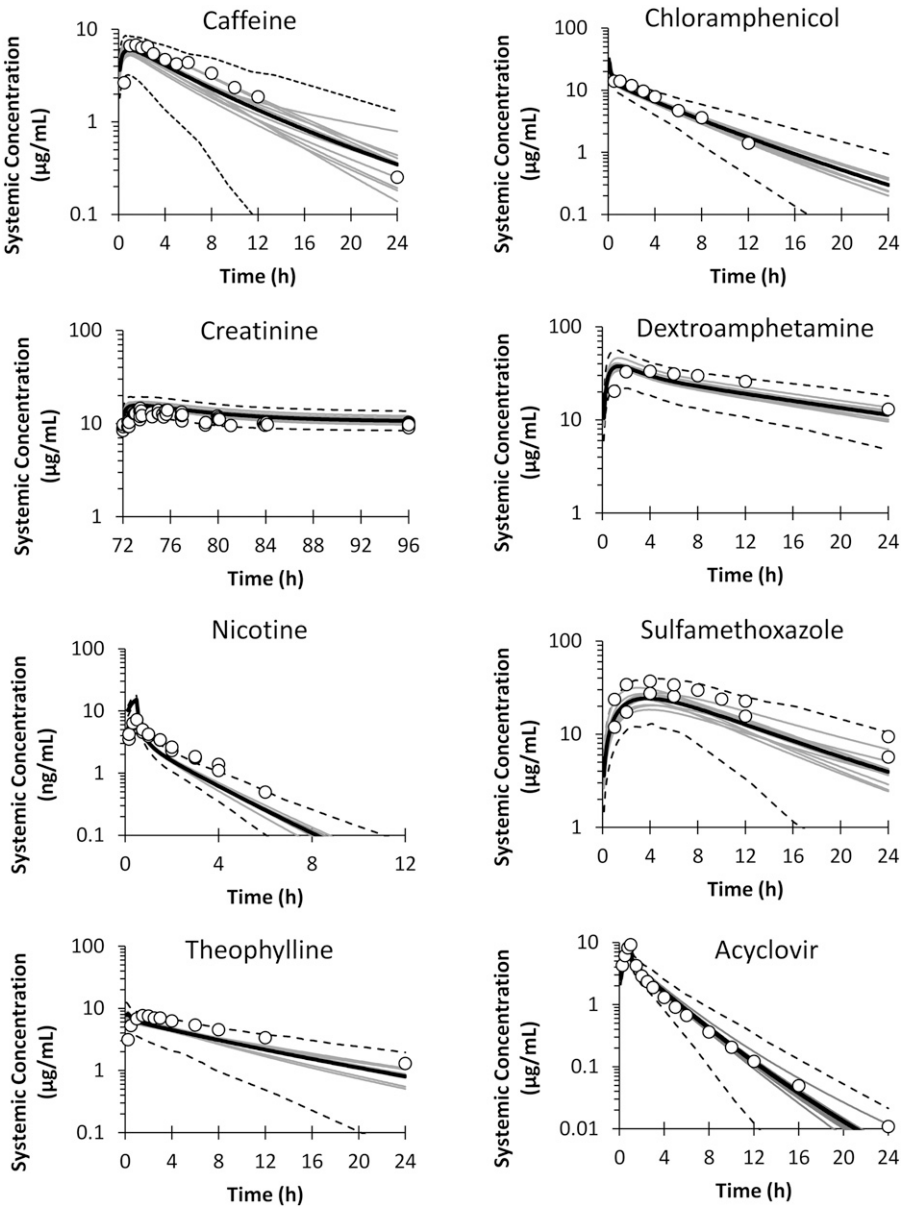

Fig. 2. Representative simulated plasma concentration-time profiles using PBPK models with MechKiM at a urine pH of 6.2. Bold black lines and dashed lines represent mean and 5th–95th percentile of 10 trials, respectively. Symbols indicate observed data.

and Morris, 2015; Burt et al., 2016; Scotcher et al., 2017). Models developed for the purpose of describing passive tubular reabsorption have allowed simulation of urine flow–dependent CL_R of drugs with different permeability properties (Tang-Liu et al., 1983; Komiya, 1986; Mayer et al., 1988); however, these models did not account for the varying physiology of the renal tubule in a mechanistic and quantitative manner and therefore lack the ability to simulate intra-tubular drug concentrations. Whereas a mechanistic kidney model implemented within the whole-body PBPK model in the Simcyp simulator could, in principle, overcome such limitations, the utility of this model for prediction of tubular reabsorption and effects of physiologic changes in urine flow and pH has not been demonstrated so far (Neuhoff et al., 2013).

In the current study, passive permeability parameters of the mechanistic kidney model were informed by IVIVE by adapting the scaling approach and regional tubular surface areas, as described previously (Scotcher et al., 2016b). Although analysis of the current data set showed a tendency for underprediction of observed CL_R, such mis-predictions are expected to have marginal consequence on the systemic exposure, as extensively reabsorbed drugs are often cleared mainly by nonrenal routes. Furthermore, apparently large differences in predicted and observed CL_R rates for extensively reabsorbed compounds can arise from only minor mispredictions of the fraction reabsorbed (Supplemental Table S15). For example, underprediction of F_{reab} of 0.99 by 1% (i.e., predicted F_{reab} of 0.98) results in 2-fold overprediction of CL_R for a completely unbound drug. For average conditions, overall CL_R predictions at pH 6.2 (AAFE of 2.87) were more accurate than the assumption of urinary pH of 7.4 (AAFE of 3.62; Table 3), although nicotine was an exception to this trend (Supplemental Table S14). A more thorough evaluation of the IVIVE predictive performance of the mechanistic kidney model, with a larger data set of drugs, is required to confirm the trends observed here. Despite this discrepancy, predicted

Downloaded from jpet.aspetjournals.org at ASPET Journals on March 13, 2024

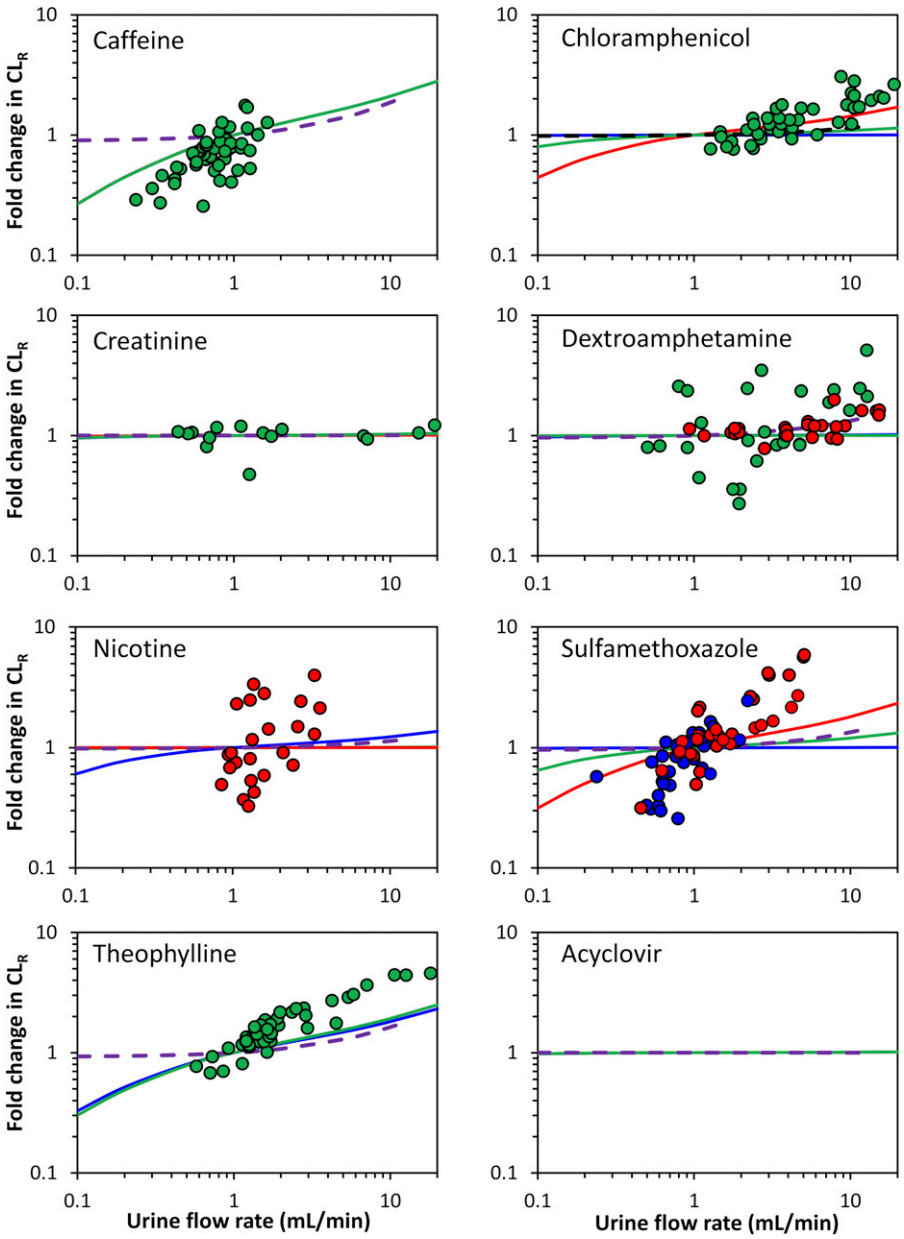

Fig. 3. Effect of urine flow on predicted CL_R in virtual population representative at a tubule pH of 4.5 (red line), 6.2 (green line), and 8.0 (blue line) using MechKiM. Purpled dashed line represents predicted CL_R using the static model for comparison. Symbols indicate observed data with a urine pH of normal (green), acidic (red), and alkaline (blue) conditions. Fold change in simulated CL_R (lines) of drugs was calculated using simulated CL_R at urine flow = 1 ml/min as baseline for each drug. The literature references for observed data are listed in Supplemental Table S10.

CL_R for nicotine at both pH levels were within 3-fold of observed data.

Prediction of CL_R using the static reabsorption model showed lower bias compared with MechKiM, despite using the same IVIVE scaling factors. The difference between the models may arise from different physiologic assumptions of each model, for example, MechKiM accounts for permeability across cell membranes, whereas static model considers permeability across epithelial cell monolayer; however, the static model has limited ability to simulate concentration-time profiles in renal tubules or account for compound ionization and permeability of different ionized species (Scotcher et al., 2016b).

The choice of in vitro permeability assay may be another consideration when evaluating the ability of kidney models to predict CL_R and F_{reab} (Kunze et al., 2014; Scotcher et al., 2016b; Mathialagan et al., 2017). Colon-derived Caco-2 and other in vitro cell lines differ from heterogeneous epithelial cells constituting the nephron tubule in terms of tight junctions (affecting para-cellular drug permeability), transporter expression, and presence of microvilli. To address the latter, one study used an empirical surface-area scaling factor to recapitulate CL_R from in vitro permeability data using a 35-compartment model (Huang and Isoherranen, 2018). No empirical scaling factor was applied in the current study; instead, the IVIVE approach relied on physiologic assumptions, although verification of each of the specific parameter values has not yet been achieved.

The mechanistic kidney model accurately identified drugs that exhibit urine flow– dependent CL_R, despite underprediction trends of the magnitude of the effect evident in some cases (Fig. 3). These underpredictions are likely related to the underprediction of the F_{reab} as discussed already herein. The model predicted that the CL_R for drugs with higher

Downloaded from jpet.aspetjournals.org at ASPET Journals on March 13, 2024

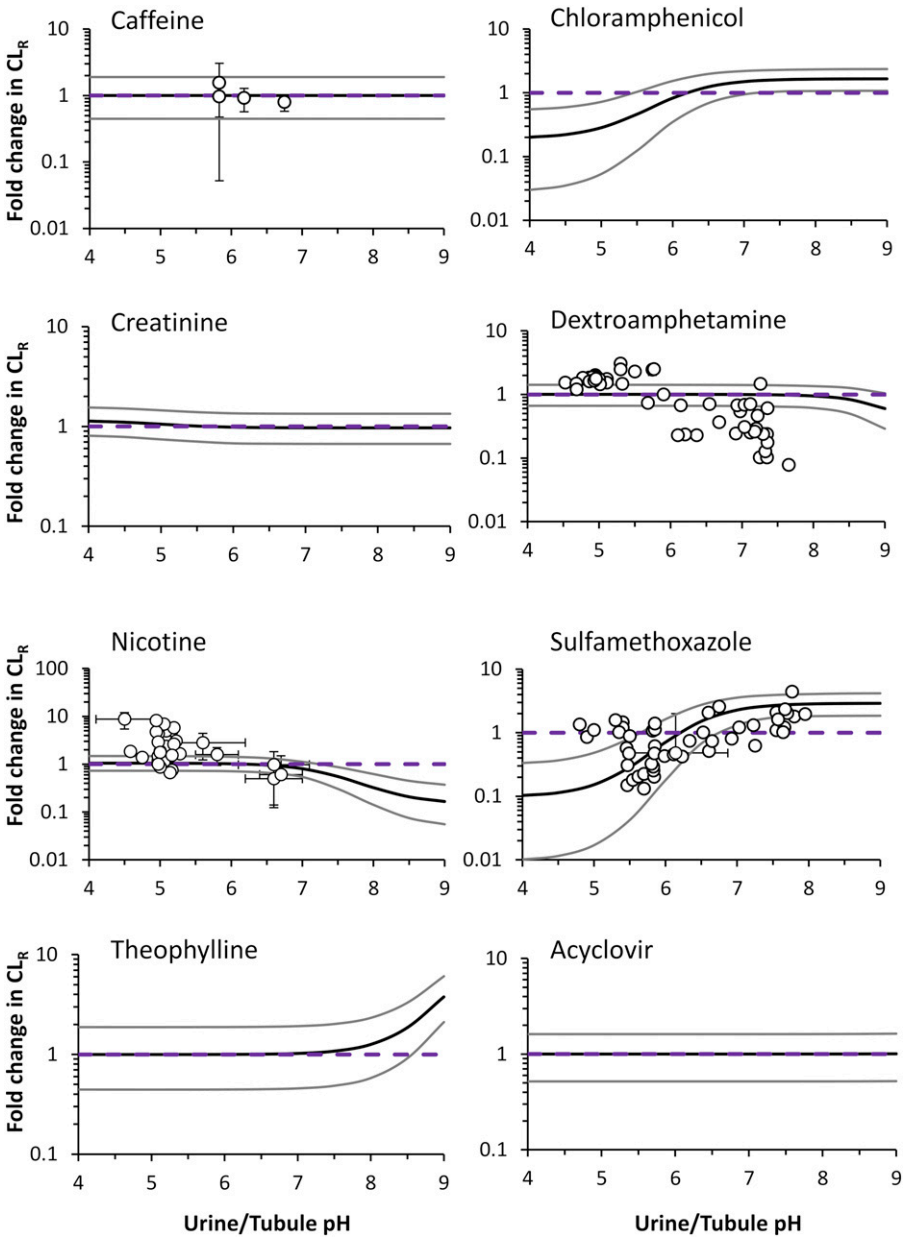

Fig. 4. Effect of urine pH on predicted CL_R in a virtual healthy population (10 trials of 10 subjects) using MechKiM. Black and gray lines represent mean and 5th–95th percentile of 100 subjects, respectively. Purpled dashed line represents predicted CL_R using the static model for comparison. Symbols indicate observed data for individuals or each study (mean ± S.D.). The literature references for observed data are listed in Supplemental Table S10.

permeability would be the most sensitive to changes in urine flow, in agreement with previous studies (Tang-Liu et al., 1983; Komiya, 1986; Mayer et al., 1988). Conversely, a negligible effect of urine flow on CL_R was predicted for low-permeability compounds creatinine and acyclovir, in agreement with clinically reported data for creatinine (Tang-Liu et al., 1983). Although previously published kidney models have been able to capture the relationship between urine flow and CL_R by fitting the model to observed data ("top-down" approach), they lacked the ability to simulate local concentrations in tubules (Tang-Liu et al., 1982, 1983).

According to Henderson-Hasselbalch equations, dextroamphetamine (pKa 10.1 for base) shows a low un-ionized fraction (<1%) within a pH range of 4.5–8.0 (Supplemental Table S4). Simulated CL_R for dextroamphetamine was sensitive to changes in urine pH only at pH > 8, in contrast to observed data in which pH sensitivity occurs across a broader range (Fig. 4). Similar outcomes were found for nicotine, highlighting some uncertainty in the fraction of un-ionized across urine pH range and/or permeability of the ionized species. Measurement of intrinsic permeability of both un-ionized and ionized drug species may provide advantages over use of P_{app}; however, the former requires a more thorough experimental design and delineation of effects of assay conditions, in addition to factors like the binding of drugs to cellular proteins and lipids, organelle-specific partitioning of drugs, and transporter activities via mechanistic modeling (Neuhoff et al., 2003; Volpe, 2008; Avdeef, 2012; Zamek-Gliszczynski et al., 2013). This approach was not considered in the current study because of the disparate experimental conditions of the literature P_{app} data collated. It is also recommended that such experiments be performed in the presence of a passive permeability marker and that transporter inhibitors be used in the assay media.

Downloaded from jpet.aspetjournals.org at ASPET Journals on March 13, 2024

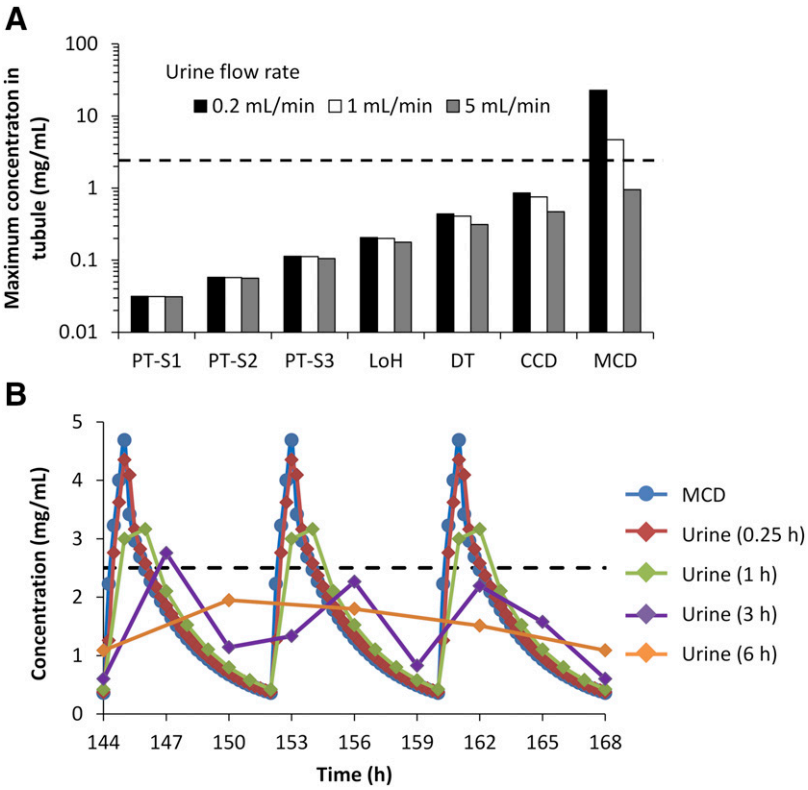

Fig. 5. Effect of urine flow on simulated renal tubular concentration of acyclovir at high-dose using MechKiM in virtual population representative. (A) Simulation of the maximum concentration of acyclovir in renal tubules after intravenously multiple administration of acyclovir at 500 mg/m^2 i.v. infusion over 60 minutes every 8 hours for 7 days at urine flow of 0.2, 1.0, and 5.0 ml/min. (B) Simulated concentration-time profiles of medullary collecting duct tubule and urine at urine flow of 1 ml/min. Urine concentrations were calculated for urine collection intervals of 0.25, 1, 3, or 6 hours. Horizontal dashed line represents the solubility of acyclovir (2.5 mg/ml).

In the current study, regional differences in filtrate pH were not considered because of the scarcity of relevant physiologic data. Micropuncture studies in rats have reported that the urine (pH 6.1) is more acidic than the proximal tubule filtrate (pH 6.7) in control conditions, but each of these can vary under different pathophysiologic states, such as acidosis (Malnic et al., 1972). Factors leading to an acidic urinary pH include a larger body weight, old age, and increased intake of meat (Rose et al., 2015), whereas alkaline urine was observed in patients with a urinary tract infection (Simerville et al., 2005). Clinical data show that urine pH can decrease to <5.5 in patients with chronic kidney disease (Kraut and Kurtz, 2005). In addition to tubular reabsorption, changes in filtrate pH may also affect activity of some transporters in vivo (e.g., MATE transporters); however, previous studies that used PBPK modeling to simulate the effect of renal insufficiency on pharmacokinetics of renally eliminated drugs assumed that pH of urine and tubular fluid were unaffected by disease (Hsu et al., 2014; Hsueh et al., 2018). All these findings highlight the importance of consideration of changes in urine pH and their impact on individual renal elimination processes when carrying out modeling and simulation within a PBPK framework, in particular for the prediction of drug exposure in specific patient populations.

The current study provides supporting evidence for the application of a mechanistic kidney model for simulation of drug concentrations in tubular filtrate in different regions of the nephron. Whereas data for preclinical species can be evaluated using experimental data obtained by invasive methods (e.g., micropuncture) (Senekjian et al., 1981), such data are not available for humans for ethical reasons. Therefore, indirect verification was performed using reported cases of drug-induced crystalluria-AKI. The relationship between solubility and simulated renal tubular concentration of acyclovir and sulfamethoxazole was in agreement with current clinical practices of managing the precipitation risk and the likelihood of crystal formation in MCD tubules by varying the urine flow rate and urine pH. The analysis of simulated acyclovir concentrations in MCD tubule in different scenarios indicated that urine sampling every 0.25 hour would sufficiently capture the dynamic changes of MCD tubular concentrations, in contrast to urine sampling at every 3 hours (Fig. 5B). Considering the practical difficulties of collecting urine at such short intervals, simulation of tubular concentration using the PBPK modeling can be a useful tool for identify compounds and dosing regimens that would be at risk of crystalluria-AKI. Supporting information could also be obtained from further development and application of high spatial resolution bioimaging techniques (Notohamiprodjo et al., 2011).

In conclusion, the current study implemented an IVIVE-PBPK approach for predicting the CL_R of renally excreted drugs that undergo tubular reabsorption and after changes in urine flow and urine pH. In addition, the mechanistic kidney model simulated the relationship between solubility and renal tubular concentration to rationalize and mitigate the risk of crystal-induced AKI. This comprehensive evaluation represents an additional step toward the qualification of mechanistic kidney models for studying the pharmacokinetic variability arising from different clinical scenarios and patient characteristics; however, uncertainty in the interindividual and intraindividual variability of regional tubular urine flow and tubular fluid pH remains. After further development, coupling of mechanistic kidney models for the prediction of pharmacodynamic and toxicity effects and the risk or probabilities of clinical outcomes under various scenarios are envisaged.

Downloaded from jpet.aspetjournals.org at ASPET Journals on March 13, 2024

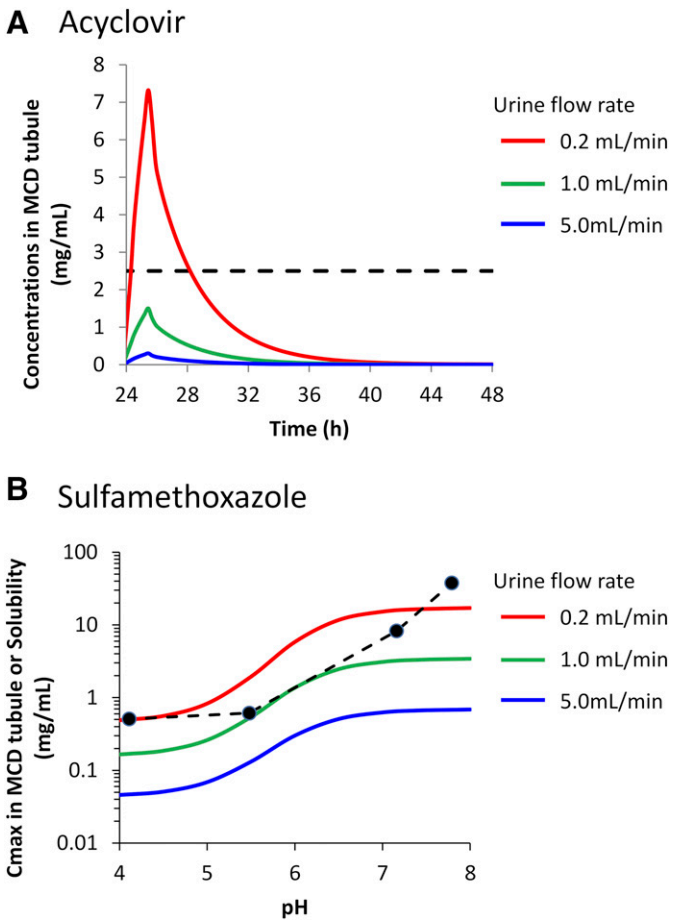

Fig. 6. Effect of urine flow and urine pH on simulated renal tubular concentration of acyclovir and sulfamethoxazole using MechKiM. (A) Effect of urine flow on simulated renal tubular concentration of low-dose acyclovir in virtual population representative. Simulated concentration-time profiles of acyclovir in medullary collecting duct tubule after 5 mg/kg i.v. infusion over 90 minutes every 24 hours for 2 days. Horizontal dashed line represents the solubility of acyclovir (2.5 mg/ml). (B) Effect of urine flow and urine pH on simulated renal tubular concentration of sulfamethoxazole in virtual population representative. Simulated concentration-time profiles of sulfamethoxazole in medullary collecting ducts tubule after oral multiple administration of sulfamethoxazole at 25 mg/kg oral administration every 6 hours for 14 days. Dashed line represents the solubility of sulfamethoxazole from the published literature (Dahlan et al., 1987).

Acknowledgments

We thank Dr. Sibylle Neuhoff and Dr. Howard Burt for expert advice and technical assistance and Eleanor Savill for help with submission.

Authorship Contributions

Participated in research design: Matsuzaki, Scotcher, Galetin, Darwich, Rostami-Hodjegan.

Performed data analysis: Matsuzaki, Scotcher, Galetin, Rostami-Hodjegan.

Wrote or contributed to the writing of the manuscript: Matsuzaki, Scotcher, Galetin, Darwich, Rostami-Hodjegan.

References

Arnal J, Gonzalez-Alvarez I, Bermejo M, Amidon GL, Junginger HE, Kopp S, Midha KK, Shah VP, Stavchansky S, Dressman JB, et al. (2008) Biowaiver monographs for immediate release solid oral dosage forms: aciclovir. *J Pharm Sci* **97**: 5061–5073.

Avdeef A (2012) *Absorption and Drug Development: Solubility, Permeability, and Charge State*, John Wiley & Sons, Hoboken, NJ.

Ball K, Jamier T, Parmentier Y, Denizot C, Mallier A, and Chenel M (2017) Prediction of renal transporter-mediated drug-drug interactions for a drug which is an OAT substrate and inhibitor using PBPK modelling. *Eur J Pharm Sci* **106**: 122–132.

Beckett AH, Salmon JA, and Mitchard M (1969) The relation between blood levels and urinary excretion of amphetamine under controlled acidic and under fluctuating urinary pH values using [14C] amphetamine. *J Pharm Pharmacol* **21**: 251–258.

Benowitz NL and Jacob P III (1993) Nicotine and cotinine elimination pharmacokinetics in smokers and nonsmokers. *Clin Pharmacol Ther* **53**:316–323.

Birkett DJ and Miners JO (1991) Caffeine renal clearance and urine caffeine concentrations during steady state dosing. Implications for monitoring caffeine intake during sports events. *Br J Clin Pharmacol* **31**:405–408.

Blanchard J and Sawers SJ (1983) Relationship between urine flow rate and renal clearance of caffeine in man. *J Clin Pharmacol* **23**:134–138.

Blum MR, Liao SH, and de Miranda P (1982) Overview of acyclovir pharmacokinetic disposition in adults and children. *Am J Med* **73**(1A):186–192.

Boroujerdi M (1982) The comparability of pharmacokinetics of creatinine in rabbit and man: a mathematical approach. *J Theor Biol* **95**:369–380.

Brigden D, Bye A, Fowle AS, and Rogers H (1981) Human pharmacokinetics of acyclovir (an antiviral agent) following rapid intravenous injection. *J Antimicrob Chemother* **7**:399–404.

Brigden D, Rosling AE, and Woods NC (1982) Renal function after acyclovir intravenous injection. *Am J Med* **73** (1A):182–185.

Burke JT, Wargin WA, Sherertz RJ, Sanders KL, Blum MR, and Sarubbi FA (1982) Pharmacokinetics of intravenous chloramphenicol sodium succinate in adult patients with normal renal and hepatic function. *J Pharmacokinet Biopharm* **10**: 601–614.

Burt HJ, Neuhoff S, Almond L, Gaohua L, Harwood MD, Jamei M, Rostami-Hodjegan A, Tucker GT, and Rowland-Yeo K (2016) Metformin and cimetidine: physiologically based pharmacokinetic modelling to investigate transporter mediated drug-drug interactions. *Eur J Pharm Sci* **88**:70–82.

Cheng Y, Vapurcuyan A, Shahidullah M, Aleksunes LM, and Pelis RM (2012) Expression of organic anion transporter 2 in the human kidney and its potential role in the tubular secretion of guanine-containing antiviral drugs. *Drug Metab Dispos* **40**:617–624.

Dahlan R, McDonald C, and Sunderland VB (1987) Solubilities and intrinsic dissolution rates of sulphamethoxazole and trimethoprim. *J Pharm Pharmacol* **39**: 246–251.

Dave RA and Morris ME (2015) Semi-mechanistic kidney model incorporating physiologically-relevant fluid reabsorption and transporter-mediated renal reabsorption: pharmacokinetics of γ-hydroxybutyric acid and L-lactate in rats. *J Pharmacokinet Pharmacodyn* **42**:497–513.

de Miranda P, Good SS, Laskin OL, Krasny HC, Connor JD, and Lietman PS (1981) Disposition of intravenous radioactive acyclovir. *Clin Pharmacol Ther* **30**:662–672.

Dolder PC, Strajhar P, Vizeli P, Hammann F, Odermatt A, and Liechti ME (2017) Pharmacokinetics and pharmacodynamics of lisdexamfetamine compared with D-amphetamine in healthy subjects. *Front Pharmacol* **8**:617.

Eck P, Silver SM, and Clark EC (1991) Acute renal failure and coma after a high dose of oral acyclovir. *N Engl J Med* **325**:1178–1179.

Felmlee MA, Dave RA, and Morris ME (2013) Mechanistic models describing active renal reabsorption and secretion: a simulation-based study. *AAPS J* **15**:278–287.

Gaohua L, Turner DB, Fisher C, Riedmaire AE, Musther H, Gardner I, and Jamei M (2016) A novel mechanistic approach to predict the steady state volume of distribution (Vss) using the Fick-Nernst-Planck equation, PAGE 25 (2016), Abstr 5709 [www.page-meeting.org/?abstract=5709].

Giustina A, Romanelli G, and Cimino A, and Brunori G (1988) Low-dose acyclovir and acute renal failure. *Ann Intern Med* **108**:312–312.

Guo Y, Chu X, Parrott NJ, Brouwer KLR, Hsu V, Nagar S, Matsson P, Sharma P, Snoeys J, Sugiyama Y, et al.; International Transporter Consortium (2018) Advancing predictions of tissue and intracellular drug concentrations using in vitro, imaging and physiologically based pharmacokinetic modeling approaches. *Clin Pharmacol Ther* **104**:865–889.

Hsu V, de L T Vieira M, Zhao P, Zhang L, Zheng JH, Nordmark A, Berglund EG, Giacomini KM, and Huang SM (2014) Towards quantitation of the effects of renal impairment and probenecid inhibition on kidney uptake and efflux transporters, using physiologically based pharmacokinetic modelling and simulations. *Clin Pharmacokinet* **53**:283–293.

Hsueh CH, Hsu V, Zhao P, Zhang L, Giacomini KM, and Huang SM (2018) PBPK modeling of the effect of reduced kidney function on the pharmacokinetics of drugs excreted renally by organic anion transporters. *Clin Pharmacol Ther* **103**:485–492.

Huang W and Isoherranen N (2018) Development of a dynamic physiologically based mechanistic kidney model to predict renal clearance. *CPT Pharmacometrics Syst Pharmacol* **7**:593–602.

Hutabarat RM, Unadkat JD, Sahajwalla C, McNamara S, Ramsey B, and Smith AL (1991) Disposition of drugs in cystic fibrosis. I. Sulfamethoxazole and trimethoprim. *Clin Pharmacol Ther* **49**:402–409.

Ito S, Kusuhara H, Kuroiwa Y, Wu C, Moriyama Y, Inoue K, Kondo T, Yuasa H, Nakayama H, Horita S, et al. (2010) Potent and specific inhibition of mMate1-mediated efflux of type I organic cations in the liver and kidney by pyrimethamine. *J Pharmacol Exp Ther* **333**:341–350.

Jamei M, Marciniak S, Edwards D, Wragg K, Feng K, Barnett A, and Rostami-Hodjegan A (2013) The simcyp population based simulator: architecture, implementation, and quality assurance. *In Silico Pharmacol* **1**:9.

Jamei M, Marciniak S, Feng K, Barnett A, Tucker G, and Rostami-Hodjegan A (2009) The Simcyp population-based ADME simulator. *Expert Opin Drug Metab Toxicol* **5**: 211–223.

Kaplan SA, Weinfeld RE, Abruzzo CW, McFaden K, Jack ML, and Weissman L(1973) Pharmacokinetic profile of trimethoprim-sulfamethoxazole in man. *J Infect Dis* **128** (Suppl):547–555.

Downloaded from jpet.aspetjournals.org at ASPET Journals on March 13, 2024

Knepper MA, Kwon T-H, and Nielsen S (2015) Molecular physiology of water balance. *N Engl J Med* **372**:1349–1358.
Komiya I (1986) Urine flow dependence of renal clearance and interrelation of renal reabsorption and physicochemical properties of drugs. *Drug Metab Dispos* **14**:239–245.
Krämer SD (2016) Quantitative aspects of drug permeation across in vitro and in vivo barriers. *Eur J Pharm Sci* **87**:30–46.
Kraut JA and Kurtz I (2005) Metabolic acidosis of CKD: diagnosis, clinical characteristics, and treatment. *Am J Kidney Dis* **45**:978–993.
Kunze A, Huwyler J, Poller B, Gutmann H, and Camenisch G (2014) In vitro-in vivo extrapolation method to predict human renal clearance of drugs. *J Pharm Sci* **103**: 994–1001.
Laskin OL, de Miranda P, King DH, Page DA, Longstreth JA, Rocco L, and Lietman PS (1982a) Effects of probenecid on the pharmacokinetics and elimination of acyclovir in humans. *Antimicrob Agents Chemother* **21**:804–807.
Laskin OL, Longstreth JA, Saral R, de Miranda P, Keeney R, and Lietman PS (1982b) Pharmacokinetics and tolerance of acyclovir, a new anti-herpesvirus agent, in humans. *Antimicrob Agents Chemother* **21**:393–398.
Lelo A, Birkett DJ, Robson RA, and Miners JO (1986) Comparative pharmacokinetics of caffeine and its primary demethylated metabolites paraxanthine, theobromine and theophylline in man. *Br J Clin Pharmacol* **22**:177–182.
Malnic G, De Mello Aires M, and Giebisch G (1972) Micropuncture study of renal tubular hydrogen ion transport in the rat. *Am J Physiol* **222**:147–158.
Männistö PT, Mäntylä R, Mattila J, Nykänen S, and Lamminsivu U (1982) Comparison of pharmacokinetics of sulphadiazine and sulphamethoxazole after intravenous infusion. *J Antimicrob Chemother* **9**:461–470.
Mathialagan S, Piotrowski MA, Tess DA, Feng B, Litchfield J, and Varma MV (2017) Quantitative prediction of human renal clearance and drug-drug interactions of organic anion transporter substrates using in vitro transport data: a relative activity factor approach. *Drug Metab Dispos* **45**:409–417.
Mayer JM, Hall SD, and Rowland M (1988) Relationship between lipophilicity and tubular reabsorption for a series of 5-alkyl-5-ethylbarbituric acids in the isolated perfused rat kidney preparation. *J Pharm Sci* **77**:359–364.
Mayersohn M, Conrad KA, and Achari R (1983) The influence of a cooked meat meal on creatinine plasma concentration and creatinine clearance. *Br J Clin Pharmacol* **15**: 227–230.
Mikami J, Oda K, and Hongo M (1975). Plasma concentration-time profile of chloramphenicol after oral, intramuscular, and intravenous administration of chloramphenicol in healthy men [in Japanese]. *Japan Soc Clin Trials Res* **3**:1862–1866.
Molander L, Hansson A, and Lunell E (2001) Pharmacokinetics of nicotine in healthy elderly people. *Clin Pharmacol Ther* **69**:57–65.
Nahata MC and Powell DA (1981) Bioavailability and clearance of chloramphenicol after intravenous chloramphenicol succinate. *Clin Pharmacol Ther* **30**:368–372.
Neuhoff S, Gaohua L, Burt H, Jamei M, Li L, Tucker GT, and Rostami-Hodjegan A (2013) Accounting for transporters in renal clearance: towards a mechanistic kidney model (Mech KiM), in *Transporters in Drug Development* (Sugiyama Y and Steffansen B eds) pp 155–177, Springer, New York.
Neuhoff S, Ungell A-L, Zamora I, and Artursson P (2003) pH-dependent bidirectional transport of weakly basic drugs across Caco-2 monolayers: implications for drug-drug interactions. *Pharm Res* **20**:1141–1148.
Newton R, Broughton LJ, Lind MJ, Morrison PJ, Rogers HJ, and Bradbrook ID (1981) Plasma and salivary pharmacokinetics of caffeine in man. *Eur J Clin Pharmacol* **21**:45–52.
Notohamiprodjo M, Pedersen M, Glaser C, Helck AD, Lodemann KP, Jespersen B, Fischereder M, Reiser MF, and Sourbron SP (2011) Comparison of Gd-DTPA and Gd-BOPTA for studying renal perfusion and filtration. *J Magn Reson Imaging* **34**: 595–607.
Perazella MA (1999) Crystal-induced acute renal failure. *Am J Med* **106**:459–465.
Posada MM, Bacon JA, Schneck KB, Tirona RG, Kim RB, Higgins JW, Pak YA, Hall SD, and Hillgren KM (2015) Prediction of renal transporter mediated drug-drug interactions for pemetrexed using physiologically based pharmacokinetic modeling. *Drug Metab Dispos* **43**:325–334.
Rodgers T, Leahy D, and Rowland M (2005) Physiologically based pharmacokinetic modeling 1: predicting the tissue distribution of moderate-to-strong bases. *J Pharm Sci* **94**:1259–1276.
Rodgers T and Rowland M (2006) Physiologically based pharmacokinetic modelling 2: predicting the tissue distribution of acids, very weak bases, neutrals and zwitterions. *J Pharm Sci* **95**:1238–1257.
Rose C, Parker A, Jefferson B, and Cartmell E (2015) The characterization of feces and urine: a review of the literature to inform advanced treatment technology. *Crit Rev Environ Sci Technol* **45**:1827–1879.
Rovei V, Chanoine F, and Strolin Benedetti M (1982) Pharmacokinetics of theophylline: a dose-range study. *Br J Clin Pharmacol* **14**:769–778.
Sawyer MH, Webb DE, Balow JE, and Straus SE (1988) Acyclovir-induced renal failure. Clinical course and histology. *Am J Med* **84**:1067–1071.
Scotcher D, Jones C, Posada M, Rostami-Hodjegan A, and Galetin A (2016a) Key to opening kidney for in vitro-in vivo extrapolation entrance in health and disease: part I: in vitro systems and physiological data. *AAPS J* **18**:1067–1081.
Scotcher D, Jones C, Rostami-Hodjegan A, and Galetin A (2016b) Novel minimal physiologically-based model for the prediction of passive tubular reabsorption and renal excretion clearance. *Eur J Pharm Sci* **94**:59–71.
Scotcher D, Jones CR, Galetin A, and Rostami-Hodjegan A (2017) Delineating the role of various factors in renal disposition of digoxin through application of physiologically based kidney model to renal impairment populations. *J Pharmacol Exp Ther* **360**:484–495.
Senekjian HO, Knight TF, and Weinman EJ (1981) Micropuncture study of the handling of gentamicin by the rat kidney. *Kidney Int* **19**:416–423.
Sharpstone P (1969) The renal handling of trimethoprim and sulphamethoxazole in man. *Postgrad Med J* **45**:38–42.
Simerville JA, Maxted WC, and Pahira JJ (2005) Urinalysis: a comprehensive review. *Am Fam Physician* **71**:1153–1162.
Soul-Lawton J, Seaber E, On N, Wootton R, Rolan P, and Posner J (1995) Absolute bioavailability and metabolic disposition of valaciclovir, the L-valyl ester of acyclovir, following oral administration to humans. *Antimicrob Agents Chemother* **39**: 2759–2764.
Takeda M, Khamdang S, Narikawa S, Kimura H, Kobayashi Y, Yamamoto T, Cha SH, Sekine T, and Endou H (2002) Human organic anion transporters and human organic cation transporters mediate renal antiviral transport. *J Pharmacol Exp Ther* **300**:918–924.
Tang-Liu DD, Tozer TN, and Riegelman S (1983) Dependence of renal clearance on urine flow: a mathematical model and its application. *J Pharm Sci* **72**: 154–158.
Tang-Liu DD-S, Tozer TN, and Riegelman S (1982) Urine flow-dependence of theophylline renal clearance in man. *J Pharmacokinet Biopharm* **10**:351–364.
Tanihara Y, Masuda S, Sato T, Katsura T, Ogawa O, and Inui K (2007) Substrate specificity of MATE1 and MATE2-K, human multidrug and toxin extrusions/H(+)-organic cation antiporters. *Biochem Pharmacol* **74**:359–371.
Tsamandouras N, Dickinson G, Guo Y, Hall S, Rostami-Hodjegan A, Galetin A, and Aarons L (2015) Development and application of a mechanistic pharmacokinetic model for simvastatin and its active metabolite simvastatin acid using an integrated population PBPK approach. *Pharm Res* **32**:1864–1883.
Tucker GT (1981) Measurement of the renal clearance of drugs. *Br J Clin Pharmacol* **12**:761–770.
Tucker WE Jr. (1982) Preclinical toxicology profile of acyclovir: an overview. *Am J Med* **73** (1A):27–30.
Tucker WE Jr., Macklin AW, Szot RJ, Johnston RE, Elion GB, de Miranda P, and Szczech GM (1983) Preclinical toxicology studies with acyclovir: acute and subchronic tests. *Fundam Appl Toxicol* **3**:573–578.
Varma MV, Feng B, Obach RS, Troutman MD, Chupka J, Miller HR, and El-Kattan A (2009) Physicochemical determinants of human renal clearance. *J Med Chem* **52**: 4844–4852.
Volpe DA (2008) Variability in Caco-2 and MDCK cell-based intestinal permeability assays. *J Pharm Sci* **97**:712–725.
Wan SH, Matin SB, and Azarnoff DL (1978) Kinetics, salivary excretion of amphetamine isomers, and effect of urinary pH. *Clin Pharmacol Ther* **23**:585–590.
Watanalumlerd P, Christensen JM, and Ayres JW (2007) Pharmacokinetic modeling and simulation of gastrointestinal transit effects on plasma concentrations of drugs from mixed immediate-release and enteric-coated pellet formulations. *Pharm Dev Technol* **12**:193–202.
Welling PG, Craig WA, Amidon GL, and Kunin CM(1973) Pharmacokinetics of trimethoprim and sulfamethoxazole in normal subjects and in patients with renal failure. *J Infect Dis* **128**(Suppl):556–566.
Ye J, Liu Q, Wang C, Meng Q, Peng J, Sun H, Kaku T, and Liu K (2012) Inhibitory effect of JBP485 on renal excretion of acyclovir by the inhibition of OAT1 and OAT3. *Eur J Pharm Sci* **47**:341–346.
Ye J, Liu Q, Wang C, Meng Q, Sun H, Peng J, Ma X, and Liu K (2013) Benzylpenicillin inhibits the renal excretion of acyclovir by OAT1 and OAT3. *Pharmacol Rep* **65**:505–512.
Yoshida K, Zhao P, Zhang L, Abernethy DR, Rekić D, Reynolds KS, Galetin A, and Huang S-M (2017) In vitro-in vivo extrapolation of metabolism- and transporter-mediated drug-drug interactions-overview of basic prediction methods. *J Pharm Sci* **106**:2209–2213.
Zamek-Gliszczynski MJ, Lee CA, Poirier A, Bentz J, Chu X, Ellens H, Ishikawa T, Jamei M, Kalvass JC, Nagar S, et al.; International Transporter Consortium (2013) ITC recommendations for transporter kinetic parameter estimation and translational modeling of transport-mediated PK and DDIs in humans. *Clin Pharmacol Ther* **94**:64–79.
Zevin S, Jacob P III, and Benowitz N (1997) Cotinine effects on nicotine metabolism. *Clin Pharmacol Ther* **61**:649–654.

Address correspondence to: Amin Rostami-Hodjegan, Centre for Applied Pharmacokinetic Research, The University of Manchester, Stopford Building, Oxford Road, Manchester M13 9PT, United Kingdom. E-mail: amin.rostami@manchester.ac.uk

Downloaded from jpet.aspetjournals.org at ASPET Journals on March 13, 2024

Journal of Pharmacology and Experimental Therapeutics

JPET/2018/251413

Supplemental Material for the manuscript:

Towards Further Verification of Physiologically-Based Kidney Models: Predictability of the Effects of Urine-Flow and Urine-pH on Renal Clearance

Takanobu Matsuzaki, Daniel Scotcher, Adam S. Darwich, Aleksandra Galetin, and Amin Rostami-Hodjegan

Centre for Applied Pharmacokinetic Research, University of Manchester, Manchester, UK (T.M., D.S., A.S.D., A.G., A.R.-H.).

Research Laboratories for Development, Shionogi & Co., Ltd., Osaka, Japan (T.M.)

Simcyp Limited (A Certara Company), Sheffield, UK (A.R.-H.)

Table S-1 Simcyp input parameters in initial PBPK model without MechKiM.

Parameter	Caffeine		Chloramphenicol		Creatinine	
MW	192.19	Simcyp default	323.13	DrugBank (1)	113.12	DrugBank (1)
LogP	-0.07	Simcyp default	1.14	DrugBank (1)	-1.76	
Compound type [a]	Monoprotic base	Simcyp default	Monoprotic acid		Monoprotic base	
pKa1	1.05 (base)	Simcyp default	5.5 (acid)	Martindale (1989) (2)	5.02 (base)	Toth (2014) (3)
pKa2	N/A		N/A		N/A	
B/P	0.977	Simcyp default	1	Assumed	0.55	Assumed
fu	0.68	Simcyp default	0.469	Koup (1979) (4)	1	No protein binding
Absorption model	1st-order	Simcyp default	N/A		1st-order	
fa	1	Simcyp default	N/A		1	
ka (1/h)	2.18	Simcyp default	N/A		1	Assumed
Qgut (L/h)	Predicted	Simcyp default	N/A		Predicted	
Permeability system	Caco2, 7.4:7.4 Passive & active	Simcyp default	N/A		Caco2, 7.4:7.4 Passive & active	
Permeability ($\times 10^{-6}$ cm/s)	30.8	Simcyp default	N/A		1.08	Mean value Matsson (2005) (5) Karlsson (1999) (6) Tavelin (2003) (7)
Permeability scalar	1.907	Simcyp default	N/A		1	
Distribution model	Full PBPK		Full PBPK		Full PBPK	
Prediction method	Method 3		Method 3		Method 3	
Kp scalar	1.1	Optimized	5	Optimized	1	
Vss (L/kg)	0.43	0.45 (Simcyp default value)	0.8	0.807 ± 0.180 Burke (1982) (8)	0.49	0.624Total body water Valentin (2002) (9)
Elimination model	Enzyme kinetics	Simcyp default	Enzyme kinetics		Enzyme kinetics	
CYP, recombinant	See supplemental Table S-2	Simcyp default	N/A		N/A	
Additional $CL_{int,HLM}$ (µL/min/mg protein)	N/A		7.51	Back-calculate from CLiv and CL_R	N/A	
fu,mic	N/A		1	Assumed	N/A	
CLiv (L/h)	CLpo 5.6	Simcyp default	13.7	Burke (1982) (8)	7.2	GFR 120 mL/min (assumed)
CL_R (L/h)	0.038	Simcyp default	1.69	Burke (1982) (8)	7.2	GFR 120 mL/min (assumed)

CL_R values for initial PBPK models before activation of MechKiM, derived from clinical data. B/P, blood to plasma partition ratio; CLint, intrinsic clearance; CL_R, renal clearance; fa, fraction absorbed; fu fraction unbound in plasma; fu,mic, fraction unbound in microsomes; ka, absorption rate constant; Kp, tissue to plasma partition coefficient; log P, logarithm of the octanol-water partition coefficient; pKa, acid dissociation constant; Qgut hybrid parameter of blood flow and drug permeability; Vss, volume of distribution at steady state.

[a] Compound type indicates the potential ionisation of the compound, not necessarily the predominant species at a particular pH.

Table S-1 (Continued) Simcyp input parameters in initial PBPK model without MechKiM.

Parameter	Dextroamphetamine		Nicotine		Sulfamethoxazole	
MW	135.21	DrugBank (1)	162.23	DrugBank (1)	253.28	DrugBank (1)
LogP	1.76	DrugBank (1)	1.17	DrugBank (1)	0.89	DrugBank (1)
Compound type [a]	Monoprotic base		Diprotic base		Ampholyte	
pKa1	10.1 (base)	Perrin (1965) (10)	3.1 (base)	Barlow (1962) (11)	5.6 (acid)	Chen (2011) (12)
pKa2	N/A		8.01 (base)	Barlow (1962) (11)	1.7 (base)	Chen (2011) (12)
B/P	1.31	Simcyp Predicted	1.23	Simcyp Predicted	0.74	Eatman (1977) (13)
fu	0.81	Weighted mean Franksson (1970) (14) Baggot (1972) (15)	0.951	Benowitz (1982) (16)	0.35	Scotcher (2016) (17)
Absorption model	1st-order		N/A		1st-order	
fa	1		N/A		0.83	Estimated from Welling (1973) (18)
ka (1/h)	0.744	Watanalumlerd (2007) (19)	N/A		0.44	Estimated from Weilling (1973) (18)
Qgut (L/h)	Predicted		N/A		Predicted	
Permeability system	Caco2, 7.4:7.4 Passive & active	Skolnik (2010) (20)	N/A		Caco-2, 6.5:7.4 Passive	Scotcher (2016) (17)
Permeability ($\times 10^{-6}$ cm/s)	40.4	Skolnik (2010) (20)	N/A		41.7	Scotcher (2016) (17)
Permeability scalar	1		N/A		1	
Distribution model	Full PBPK		Full PBPK		Full PBPK	
Prediction method	Method 3		Method 3		Method 3	
Kp scalar	0.38	Optimized	0.34	Optimized	1.3	Optimized
Vss (L/kg)	3.4	3.52 Watanalumlerd (2007) (19)	1.5	2.8 ± 0.9 Benowitz (1993) (21)	0.175	0.21 Mannisto (1982) (22)
Elimination model	Enzyme kinetics		Enzyme kinetics		Enzyme kinetics	
CYP, recombinant	N/A		N/A		N/A	
Additional $CL_{int,HLM}$ (µL/min/mg protein)	1.55	Back-calculate from CLiv and CL_R	61.1	Back-calculated from CLiv and CL_R	0.722	Back-calculate from CLiv and CL_R
fu,mic	1	Assumed	1	Assumed	1	Assumed
CLiv (L/h)	CLpo 16.5	Watanalumlerd (2007) (19)	78.42	Molander (2001) (23)	1.28	Manissto (1982) (22)
CL_R (L/h)	5.44	Becket (1969) (24)	3.78	Molander (2001) (23)	0.3	Manissto (1982) (22)

CL_R values for initial PBPK models before activation of MechKiM, derived from clinical data. B/P, blood to plasma partition ratio; CLint, intrinsic clearance; CL_R, renal clearance; fa, fraction absorbed; fu fraction unbound in plasma; fu,mic, fraction unbound in microsomes; ka, absorption rate constant; Kp, tissue to plasma partition coefficient; log P, logarithm of the octanol-water partition coefficient; pKa, acid dissociation constant; Qgut hybrid parameter of blood flow and drug permeability; Vss, volume of distribution at steady state.
[a] Compound type indicates the potential ionisation of the compound, not necessarily the predominant species at a particular pH.

Table S-1 (Continued) Simcyp input parameters in initial PBPK model without MechKiM.

Parameter	Theophylline		Acyclovir	
MW	180.2	Simcyp default	225.2	DrugBank (1)
LogP	-0.02	Simcyp default	-1.56	DrugBank (1)
Compound type [a]	Ampholyte	Simcyp default	Ampholyte	
pKa1	8.8 (acid)	Simcyp default	9.25 (acid)	ZOVIRAX Label
pKa2	0.99 (base)	Simcyp default	2.27 (base)	ZOVIRAX Label
B/P	0.815	Simcyp default	1	de Milanda (1981) (25)
fu	0.5	Simcyp default	0.846	de Milanda (1981) (25)
Absorption model	1st-order	Simcyp default	N/A	
fa	1	Simcyp default	N/A	
ka (1/h)	6	Simcyp default	N/A	
Qgut (L/h)	Predicted	Simcyp default	N/A	
Permeability system	Caco2, 7.4:7.4 Passive & active	Simcyp default	N/A	
Permeability ($\times 10^{-6}$ cm/s)	25.0	Simcyp default	N/A	
Permeability scalar	1.5	Simcyp default	N/A	
Distribution model	Full PBPK		Full PBPK	
Prediction method	Method 3		Method 3	
Kp scalar	1.6	Optimized	1.7	Optimized
Vss (L/kg)	0.46	0.475 (Simcyp default value)	0.72	0.71 Blum (1982) (26)
Elimination model	Enzyme kinetics	Simcyp default	Enzyme kinetics	
CYP, recombinant	See supplemental Table S-2	Simcyp default	N/A	
Additional $CL_{int,HLM}$ (µL/min/mg protein)	N/A		1.49	Back-calculate from CLiv and CL_R
fu,mic	N/A		1	Assumed
CLiv (L/h)	CLpo 3.5	Simcyp default	19.6	Blum (1982) (26)
CL_R (L/h)	0.31	Simcyp default	14.9	Blum (1982) (26)

CL_R values for initial PBPK models before activation of MechKiM, derived from clinical data. B/P, blood to plasma partition ratio; CLint, intrinsic clearance; CL_R, renal clearance; fa, fraction absorbed; fu fraction unbound in plasma; fu,mic, fraction unbound in microsomes; ka, absorption rate constant; Kp, tissue to plasma partition coefficient; log P, logarithm of the octanol-water partition coefficient; N/A, not applicable; pKa, acid dissociation constant; Qgut hybrid parameter of blood flow and drug permeability; Vss, volume of distribution at steady state.

[a] Compound type indicates the potential ionisation of the compound, not necessarily the predominant species at a particular pH.

Table S-2 Enzyme kinetic parameters used for caffeine and theophylline in initial PBPK model without MechKiM. The parameters were obtained from existing Simcyp compound files (Simcyp version 16.1; Sim-Caffeine and SV-Theophylline).

	Caffeine	Theophylline
Pathway	N1-demethylation	N1-demethylation
Enzyme	CYP1A2	CYP1A2
Vmax (µmol/ min/ pmol of isoform)	0.56	2.47
Km (µM)	157	1080
CLint (µL/ min/ pmol of isoform)	N/A	N/A
fu,mic	1	1
Pathway	N1-demethylation	N3-demethylation
Enzyme	CYP2E1	CYP1A2
Vmax (µmol/ min/ pmol of isoform)	0.03	6
Km (µM)	1411	377
fu,mic	1	1
Pathway	N3-demethylation	N3-demethylation
Enzyme	CYP1A2	CYP2D6
Vmax (µmol/ min/ pmol of isoform)	13.6	1.8
Km (µM)	30	6897
fu,mic	1	1
Pathway	N7-demethylation	8-OH
Enzyme	CYP1A2	CYP1A2
Vmax (µmol/ min/ pmol of isoform)	0.21	4.11
Km (µM)	245	394
fu,mic	1	1
Pathway	N7-demethylation	8-OH
Enzyme	CYP2E1	CYP2D6
Vmax (µmol/ min/ pmol of isoform)	0.02	4.68
Km (µM)	823	10709
fu,mic	1	1
Pathway	OH	8-OH
Enzyme	CYP1A2	CYP2E1
Vmax (µmol/ min/ pmol of isoform)	0.36	40.78
Km (µM)	265	16855
fu,mic	1	1
Pathway	OH	8-OH
Enzyme	CYP2E1	CYP3A4
Vmax (µmol/ min/ pmol of isoform)	0.18	0.4
Km (µM)	1019	23393
fu,mic	1	1
Pathway	OH	N/A
Enzyme	CYP3A4	N/A
Vmax (µmol/ min/ pmol of isoform)	1.8	N/A
Km (µM)	45080	N/A
fu,mic	1	N/A

fu,mic, fraction unbound in microsomes; Km, Michaelis-Menten constant; Vmax, maximum rate of metabolism.

Table S-3 Apparent permeability in Caco-2 cell monolayers collected from literature.

Compound	Caco-2 P_{app} ($\times 10^{-6}$ cm/s)	pH condition (apical:basal)	Comment	Reference
Caffeine	81.1	6.5:7.4	presence of an efflux transporter inhibitor cocktail (50 μM quinidine, 20 μM sulfasalazine, 100 μM benzbromarone)	Scotcher (2016) (17)
Chloramphenicol	20.6	6.5:7.4	-	Yee (1997) (27)
Creatinine	1.08	7.4:7.4	mean value of 3 different studies	Matsson (2005) (5) Karlsson (1999) (6) Tavelin (2003) (7)
Dextroamphetamine	40.35	7.4:7.4	-	Skolnik (2010) (20)
Nicotine	19.4	7.4:7.4	-	Yazdanian (1998) (28)
Sulfamethoxazole	41.7	6.5:7.4	presence of an efflux transporter inhibitor cocktail (50 μM quinidine, 20 μM sulfasalazine, 100 μM benzbromarone)-	Scotcher (2016) (17)
Theophylline	65.13	6.5:7.4	presence of an efflux transporter inhibitor cocktail (50 μM quinidine, 20 μM sulfasalazine, 100 μM benzbromarone)	Scotcher (2016) (17)
Acyclovir	0.291	6.8:7.4	weighted mean value of 3 experiments	Parr (2016) (29)

P_{app}, apparent permeability.

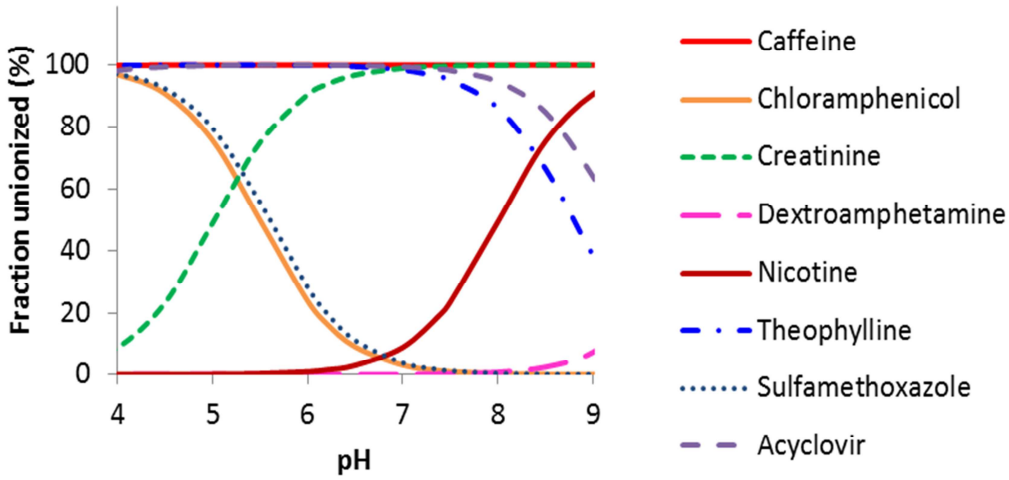

Figure S-1 Fraction of unionised form based on Henderson–Hasselbalch equations.

Table S-4 Fraction of unionised form based on Henderson–Hasselbalch equations.

Compounds	Fraction of unionized form					
	pH 4.5 [a]	pH 6.2 [b]	pH 6.5	pH 6.8	pH 7.4 [c]	pH 8.0 [d]
Caffeine	1.00	1.00	1.00 [e]	1.00	1.00	1.00
Chloramphenicol	0.91	0.17	0.09 [e]	0.05	0.01	0.00
Creatinine	0.23	0.94	0.97	0.98	1.00 [e]	1.00
Dextroamphetamine	0.00	0.00	0.00	0.00	0.00 [e]	0.01
Nicotine	0.00	0.02	0.03	0.06	0.20 [e]	0.49
Sulfamethoxazole	0.92	0.20	0.11 [e]	0.06	0.02	0.00
Theophylline	1.00	1.00	1.00 [e]	0.99	0.96	0.86
Acyclovir	0.99	1.00	1.00	1.00 [e]	0.99	0.95

[a] Assuming urine was under acidic condition.
[b] Assuming as average pH condition of urine.
[c] Default value of urine and tubule fluid pH in Simcyp. Basolateral pH in Caco-2 P_{app} used in this study.
[d] Assuming urine was under alkaline condition.
[e] Apical pH in Caco-2 P_{app} used in this study.

Table S-5 Tubular surface area for each tubular section (Reference: Scotcher 2016 (17))

	PT	LoH	DT	CCD [a]	MCD [a]
Length (mm)	18	12	5.5	10	12
Diameter (µm)	60	18	50	50	[40 - 200] [b]
Number nephrons / kidney	900000	900000	900000	90,000	90000 - 250
Surface area (m^2) [c]	6.11	0.16	0.21	0.04	0.008 [d]

PT, Proximal tubule; LoH, Loop of Henle; DT, Distal tubule; CCD, Cortical collecting duct; MCD, medullary collecting duct.
[a] Special consideration was made for the CD compartment, due to the merging of nephrons to form the cortical CD, and merging of CDs in the innermedulla. To account for this, the number of nephrons was reduced to 90,000 nephrons/kidney for the cortical and outer medulla CD, with surface area calculated following assumption of a cylinder.
[b] Diameter of collecting ducts changes between cortex and outer medulla (50 µm), and the inner medulla. Within the inner medulla, as the collecting ducts progress toward the apex, number of collecting ducts reduces, while the diameter of the collecting ducts increase (from 40 to 200 µm).
[c] Tubular surface area of the PT, LoH and DT were recalculated using the highest and lowest values collated for the length and diameter of these tubular sections, assuming 900,000 nephrons per kidney. The surface area for collecting duct was consistent with the assumptions of 90,000 cylindrical tubules per kidney, which accounts for the merging of nephrons to join the cortical collecting duct, and the branching structure of the collecting duct in the inner medulla. Surface area values were also recalculated with correction for microvilli related surface area (7.5-fold) for the LoH, DT and CD sections.
[d] The surface area of the inner medulla CD was calculated using an exponential function shown in following equation which accounts for the concomitant decrease in number and increase in diameter of CD, as they traverse towards the renal pelvis

$$C_x = (d_0 \times NCD_0 \times \pi) e^{\left(\left(\frac{x \times F}{n}\right) \times \ln\left(\frac{2}{\frac{d_0}{d_n}^{\frac{1}{F}}} \right) \right)}$$

Where d_0 and d_n are the diameter of IMCD at the papilla apex and at the outer medulla-inner medulla boundary, NCD_0 is the number of IMCDs at the papilla apex, and F is the number of fusion events. The area under the curve as IMCD surface area was calculated by integration. Details were described previously (Scotcher 2016 (17)).

Table S-6 CL_{PD} parameters used in MechKiM.

Compound	Corrected P_{app} ($\times 10^{-6}$ cm/s)	CL_{PD} (µL/ min/ million PTC)						
		PT -1	PT -2	PT -3	LoH	DT	CCD	MCD
Caffeine	81.1	29.0	29.0	29.0	0.775	0.986	0.179	0.0364
Chloramphenicol	20.6	7.38	7.38	7.38	0.197	0.251	0.0455	0.00924
Creatinine	1.08	0.387	0.387	0.387	0.0103	0.0131	0.00239	0.000485
Dextroamphetamine	40.35	14.5	14.5	14.5	0.385	0.491	0.0892	0.0181
Nicotine	19.4	6.98	6.98	6.98	0.186	0.237	0.0431	0.00875
Sulfamethoxazole	41.7	14.9	14.9	14.9	0.398	0.507	0.0922	0.0187
Theophylline	65.13	23.3	23.3	23.3	0.622	0.792	0.144	0.0292
Acyclovir	0.291	0.104	0.104	0.104	0.00278	0.00354	0.000643	0.000131

P_{app}, apparent permeability; PTC, Proximal tubule cells; PT, Proximal tubule; LoH, Loop of Henle; DT, Distal tubule; CD, Collecting duct.

Table S-7 Physiological parameter values used for tubular compartments in the static model. (Scotcher 2016 (17))

Tubule	Tubular surface area (m^2)	Tubular flow rate (mL/min) [a]
PT	6.1	81.6 (120 - 43.2)
LoH	0.16 [b]	33.6 (43.2 - 24.0)
DT	0.21 [b]	17.8 (24.0 - 11.6)
CD	0.045 [b,c]	6.3 (11.6 - 1.0)

PT, Proximal tubule; LoH, Loop of Henle; DT, Distal tubule; CD, Collecting duct.
[a] Values represent midpoint flowrates, ranges in parenteses represent flows at beginning and end of tubule regions
[b] TSA_{LoH}, TSA_{DT} and TSA_{CD} calculated accounting for microvilli
[c] TSA_{CD} includes an exponential function for calculateing surface area of inner medulla CD.

Table S-8 Predictability of renal clearance for acyclovir using mechanistic kidney model with transporters.
For simulation, urine/tubular pH at normal condition was used as 7.4 (Simcyp default value) and 6.2 (Rose et al).

	Dose Information	Number of subjects	Observed CL_R (mL/min)	Predicted CL_R (mL/min)			Pred/Obs			Reference
				PBPK pH7.4	PBPK pH6.2	Static	PBPK pH7.4	PBPK pH6.2	Static	
Without transporters	350 mg, 1h infusion	12	283 ± 103	115 (78-162)	115 (78-163)	99.8	0.41 (0.28-0.57)	0.41 (0.28-0.58)	0.35	Soul-Lawton (1995) (30)
Refinement	350 mg, 1h infusion	12	283 ± 103	263 (138-422)	263 (138-422)	N/A	0.93 (0.49-1.49)	0.93 (0.49-1.49)	N/A	Soul-Lawton (1995) (30)
Verification	50 mg IV bolus	6	185 ± 37	256 (133-495)	256 (133-495)	N/A	1.4 (0.7-2.7)	1.4 (0.7-2.7)	N/A	Brigden (1981) (31)
	50 mg IV 1 h infusion	2	249	294 (141-549)	294 (141-549)	N/A	1.2 (0.6-2.2)	1.2 (0.6-2.2)	N/A	Brigden (1981) (31)
	50 mg IV 10 min infusion	2	117	296 (141-556)	296 (141-555)	N/A	2.5 (1.2-4.8)	2.5 (1.2-4.7)	N/A	Brigden (1981) (31)
	0.5-2.5 mg/kg, IV infusion 1h	5	240 ± 77	256 (124-439)	256 (124-439)	N/A	1.1 (0.5-1.8)	1.1 (0.5-1.8)	N/A	de Miranda (1981) (25)
	5 mg/kg, 1 h infusion	3	248 ± 46	266 (123-441)	266 (123-441)	N/A	1.1 (0.5-1.8)	1.1 (0.5-1.8)	N/A	Laskin (1982a) (32)
	2.5 mg/kg, 1h infusion over 1h	3	158 ± 19	273 (123-439)	273 (123-439)	N/A	1.7 (0.8-2.8)	1.7 (0.8-2.8)	N/A	Laskin (1982b) (33)
	5.0 mg/kg, 1h infusion over 1h	3	225 ± 100	273 (123-439)	273 (123-439)	N/A	1.2 (0.5-2)	1.2 (0.5-2)	N/A	Laskin (1982b) (33)
	10 mg/kg, 1h infusion over 1h	4	238 ± 64	273 (123-464)	273 (123-463)	N/A	1.1 (0.5-1.9)	1.1 (0.5-1.9)	N/A	Laskin (1982b) (33)
	15 mg/kg, 1h infusion over 1h	3	398 ± 67	273 (123-439)	273 (123-439)	N/A	0.69 (0.31-1.1)	0.69 (0.31-1.1)	N/A	Laskin (1982b) (33)

N/A, Not applicable.

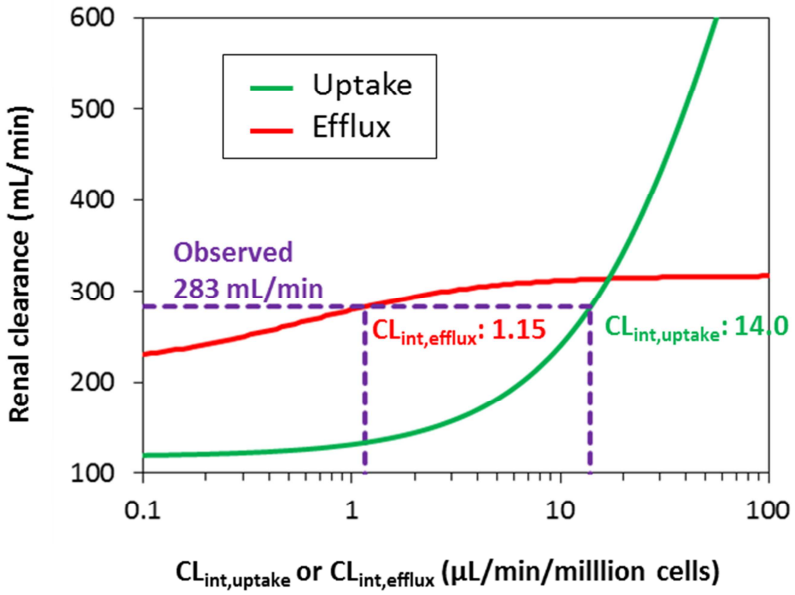

Figure S-2 Sensitivity analysis of $CL_{int,uptake}$ and $CL_{int,efflux}$ on renal clearance for acyclovir.
Observed data used for estimating $CL_{int,efflux}$ was taken from a published literature (30). For sensitivity analysis of $CL_{int,efflux}$ the $CL_{int,uptake}$ was fixed at 14.0 µL/min/million cells; for sensitivity analysis of $CL_{int,uptake}$ the $CL_{int,efflux}$ was fixed at 1.15 µL/min/million cells. $f_{u,cell}$ was fixed at 0.9988 (predicted value in Simcyp simulator).

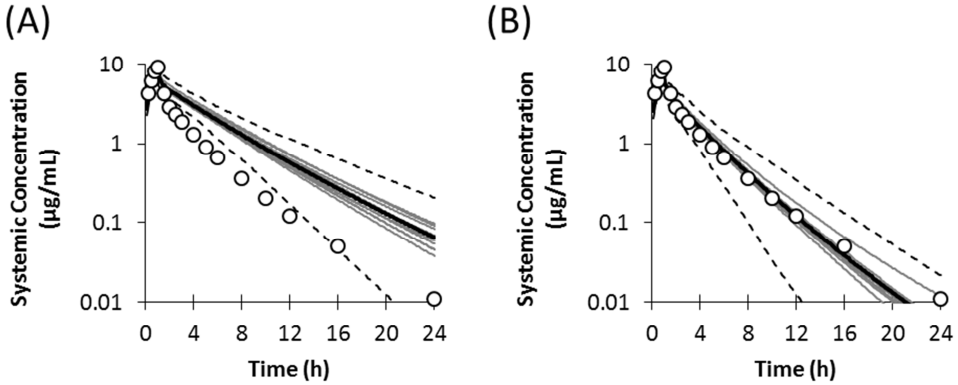

Figure S-3 Simulated plasma concentration-time profiles of acyclovir using PBPK model with MechKiM without (A) or with (B) 1 uptake and 1 efflux transporters after intravenous administration of acyclovir at 350 mg.
Bold black lines and dashed lines represent mean and 5th-95th percentile of 10 trials, respectively. Symbols indicate observed data [Soul-Lawton (1995) (30)].

Table S-9 Dosage information used to simulate the effect of urine-flow and urine pH on CL_R using MechKiM

Compound	Dosage
Caffeine	300 mg Oral SD
Chloramphenicol	1000 mg IV bolus (1 min) SD
Creatinine	18.72 mg/kg/day, 24 h infusion for 4 days
Dextroamphetamine	10 mg Oral SD
Nicotine	0.015 mg/kg IV, 0.5 h infusion, SD
Sulfamethoxazole	800 mg Oral SD
Theophylline	250 mg Oral SD
Acyclovir	350 mg IV, 1 h infusion, SD

Table S-10 Clinical trials used for evaluation of urine-flow and urine-pH dependency on CL_R using MechKiM. Basic dosage and demographic information are shown.

Compound	Reference	Dose Information	Subjects Information	Urine pH Mean ± SD (Range)	Perturbation	Urine-flow dependency on CL_R		
						Equation for fit (Y = CL_R; X = urine flow or urine pH)	R^2	Baseline CL_R at urine flow of 1 mL/min or pH 6.2 (mL/min) [a]
Caffeine	Birkett (1991) (34)	150 mg Oral TID for 6 days	3 male, 3 female, 20-22 years	N/A	Urine-flow	Y (mL/h) = 0.5X + 12.4 [b]	0.792	0.707
	Blanchard (1983) (35)	5 mg/kg Oral SD	8 male, 18-24 years	6.18	Urine-flow	Y (mL/h) = 3.053X + 45.236 [b,c]	0.572	1.56
	Blanchard (1983) (35)	5 mg/kg IV SD	8 male, 18-24 years	6.75	Urine-flow	Y (mL/h) = 3.053X + 45.236 [b,c]	0.572	1.56
	Blanchard (1983) (35)	5 mg/kg Oral SD	Elder 8 male, 66-78 years	5.83	Urine-flow	Y (mL/h) = 3.053X + 45.236 [b,c]	0.572	1.56
	Blanchard (1983) (35)	5 mg/kg IV SD	Elder 8 male, 66-78 years	5.83	Urine-flow	Y (mL/h) = 3.053X + 45.236 [b,c]	0.572	1.56
	Blanchard (1983) (35)	5 mg/kg Oral or IV SD	8 male, 18-24 years or Elder 8 male, 66-78 years	(5.83-6.75)	Urine pH	Y (mL/min) = $276.35X^{-2.975}$	0.436	1.21
Chloramphenicol	Tang-Liu (1983) (36)	Not reported	Not reported	N/A	Urine-flow	Y (mL/min) = 2.0997X + 22.077 [d,e]	0.633	24.2
Creatinine	Tang-Liu (1983) (36)	Not reported	Not reported	N/A	Urine-flow	Y (mL/min) = 0.0673X + 117.08 [e]	0.0673	Assumed same as GFR of 120 mL/min
Dextroamphetamine	Beckett (1969) (24)	8.7 mg Oral SD	2 male, 21 and 23 years	(5.5-7.7)	Urine-flow	Y (mL/min) = 9.8217X + 49.658 [e]	0.305	59.5
	Beckett (1969) (24)	8.7 mg Oral SD	2 male, 21 and 23 years	Acidic 5 ± 0.2	Urine-flow	Y (mL/min) = 12.774X + 306.73 [e]	0.422	320
	Beckett (1969) (24)	8.7 mg Oral SD	2 male, 21 and 23 years	(5.5-7.7)	Urine pH	Y (mL/ min) = −127.69X + 998.95 [e]	0.628	207
Nicotine	Feyerabend (1978) (37)	Cigarette or 2, 4 mg Chewing-gum	1 male, 38 years	Acidic (4.6-5.3)	Urine-flow	Y (mL/min) = 71.321X + 60.004 [e]	0.192	131
	Benowitz (1985) (38)	Cigarette smoking	8 male, 3 female, 28-55 years	5.8 ± 0.3	Urine-pH	Y (mL/min) = $100842X^{-4.031}$ [e]	0.230	64.5
	Benowitz (1985) (38)	Cigarette smoking	8 male, 3 female, 28-55 years	5.6 ± 0.6	Urine-pH	Y (mL/min) = $100842X^{-4.031}$ [e]	0.230	64.5
	Benowitz (1985) (38)	Cigarette smoking	8 male, 3 female, 28-55 years	Acidic 4.5 ± 0.4	Urine-pH	Y (mL/min) = $100842X^{-4.031}$ [e]	0.230	64.5
	Benowitz (1985) (38)	Cigarette smoking	8 male, 3 female, 28-55 years	Alkaline 6.7 ± 0.3	Urine-pH	Y (mL/min) = $100842X^{-4.031}$ [e]	0.230	64.5

	Molander (2001) (23)	0.028 mg/kg IV infusion for 10 min SD	10 male, 10 female, 22-43 years	6.6 ± 0.5	Urine-pH	$Y = 100842X^{-4.031}$ [e]	0.230	64.5
Sulfamethoxazole	Vree (1978) (39)	100-800 mg Oral SD	2 subjects	Acidic 5.90 (5.36 - 6.46)	Urine-flow	Y (mL/min) = 0.6503X – 0.1012 [e]	0.902	0.549
	Vree (1978) (39)	100-800 mg Oral SD	2 subjects	Alkaline 7.29 (7.01 - 7.73)	Urine-flow	Y (mL/min) = 15.644X + 0.6824 [e]	0.556	15.0
	Sharpstone (1969) (40)	800 mg Oral SD	4 subjects	Acidic (4.8-5.85)	Urine-flow	Y (mL/min) = 2.7318X + 4.2568 [e]	0.894	6.99
	Sharpstone (1969) (40)	800 mg Oral SD	4 subjects	Alkaline (6.6-7.95)	Urine-flow	Y (mL/min) = 9.3834X + 3.8075 [e]	0.465	13.2
	Hutabarat (1991) (41)	10 mg/kg IV infusion for 60 min SD	7 male, 1 female, 22-27 years	6.14 ± 0.73	Urine-pH	Y (mL/min) = 3.5329 X – 14.579 [e]	0.298	7.32
Theophylline	Tang-Liu (1982) (42)	Not reported	2 subjects, 24 - 32 years	N/A	Urine-flow	Y (mL/min) = 5.2252ln(X) + 4.3551 [e]	0.897	4.36

N/A, not applicable.

[a] Value was calculated from equation for fit.

[b] Reported equation as unit of mL/h.

[c] Equation was reported as unbound CL_R. Therefore, CL_R values were recalculated by unbound fraction.

[d] CL_R values and urine flow rate were reported as percentage of inulin clearance. CL_R values and urine flow rate were obtained by the assumed inulin clearance of 120 mL/min.

[e] Analyzed using Microsoft Excel.

Table S-11 Tubular flow rate values used in MechKiM to simulate change in urine flow rate.

Urine flow rate	Tubular inflow rate parameter value (mL/ min)				
(mL/min)	Proximal tubule	Loop of Henle [a]	Distal tubule [a]	Collecting duct [a]	Bladder
0.1	120	42.65	23.31	10.74	0.1
0.2	120	42.71	23.39	10.83	0.2
0.5	120	42.90	23.63	11.10	0.5
1.0 (default)	120	43.23	24.03	11.56	1.0
2.0	120	43.87	24.84	12.47	2.0
5.0	120	45.81	27.26	15.2	5.0
7.5	120	47.42	29.27	17.48	7.5
10.0	120	49.03	31.29	19.76	10.0
20.0	120	55.48	39.35	28.87	20.0

[a] Values were automatically recalculated by changing the flow rate at bladder, following the gradient of flow rate from proximal tubule to bladder.

Table S-12 Tubular flow rate values used in static model to simulate change in urine flow rate.

Urine flow rate	Tubular flow rate parameter value (mL/ min)				
(mL/min)	Proximal tubule [a]	Loop of Henle [a]	Distal tubule [a]	Collecting duct [a,b]	Bladder
0.1	81.6	33.6	17.8	5.85	0.1
0.2	81.6	33.6	17.8	5.90	0.2
0.5	81.6	33.6	17.8	6.05	0.5
1.0 (default)	81.6	33.6	17.8	6.30	1.0
2.0	81.6	33.6	17.8	6.80	2.0
5.0	81.6	33.6	17.8	8.30	5.0
7.5	81.6	33.6	17.8	9.55	7.5
10.0	81.6	33.6	17.8	10.8	10.0
11.6 [c]	81.6	33.6	17.8	11.6	11.6

[a] Values represent midpoint of flowrates at beginning and end of tubule regions.
[b] Values were calculated as average of flow rate (11.6 mL/min) at the beginning of collecting ducts and bladder flow rate.
[c] The highest flow rate investigated (11.6 mL/ min) was determined by the assumed flow rate at the beginning of the collecting duct.

Table S-13 Examples for changes of urine flow rate

Treatment	Urine flow rate (mL/min)		Effect on urine flow	Reference
	Maximum	Control		
Ingestion of water				
1 L of water	6.0	1.0	6-fold increase	Guyton (2004) (43)
7 mL/kg of water	3.4	1.0	3.4-fold increase	Matsukura (1979) (44)
Diuretics				
Furosemide, 40 mg	5.1	0.5	9.4-fold increase	Branch (1979) (45)
Bumetanide, 1 mg	7.3	0.4	17.8-fold increase	Branch (1979) (45)
Hydrochlorothiazide, 50 mg	3.3	1.9	1.7-fold increase	Bloomfield (1965) (46)
Tolvaptan, 60 mg	3.2	1.6	2.0-fold increase	Gheorghiade (2003) (47)
Furosemide, 80 mg	15.3	3.0	5.1-fold increase	Goldsmith (2011) (48)
Conivaptan, 20 mg	11.7	3.5	3.3-fold increase	Goldsmith (2011) (48)
Combination of furosemide and conivaptan	27.7	2.7	10.4-fold increase	Goldsmith (2011) (48)
Others				
Caffeine, 250 mg	6.0	3.6	1.7-fold increase	Nussberger (1990) (49)
Caffeine, 8.75 mL/kg	10.2	7.8	1.3-fold increase	Wemple (1997) (50)
Theophylline, 500 mg	1.3	0.7	1.8-fold increase	Nielsen (1961) (51)
Nicotine (cigaretto smoking)	-	-	decrease	Matsukura (1979) (44)
Fluid therapy				
Prevention of crystal induced acute kidney injury	1.7 to 2.5	-	-	Perazella (1999) (52)

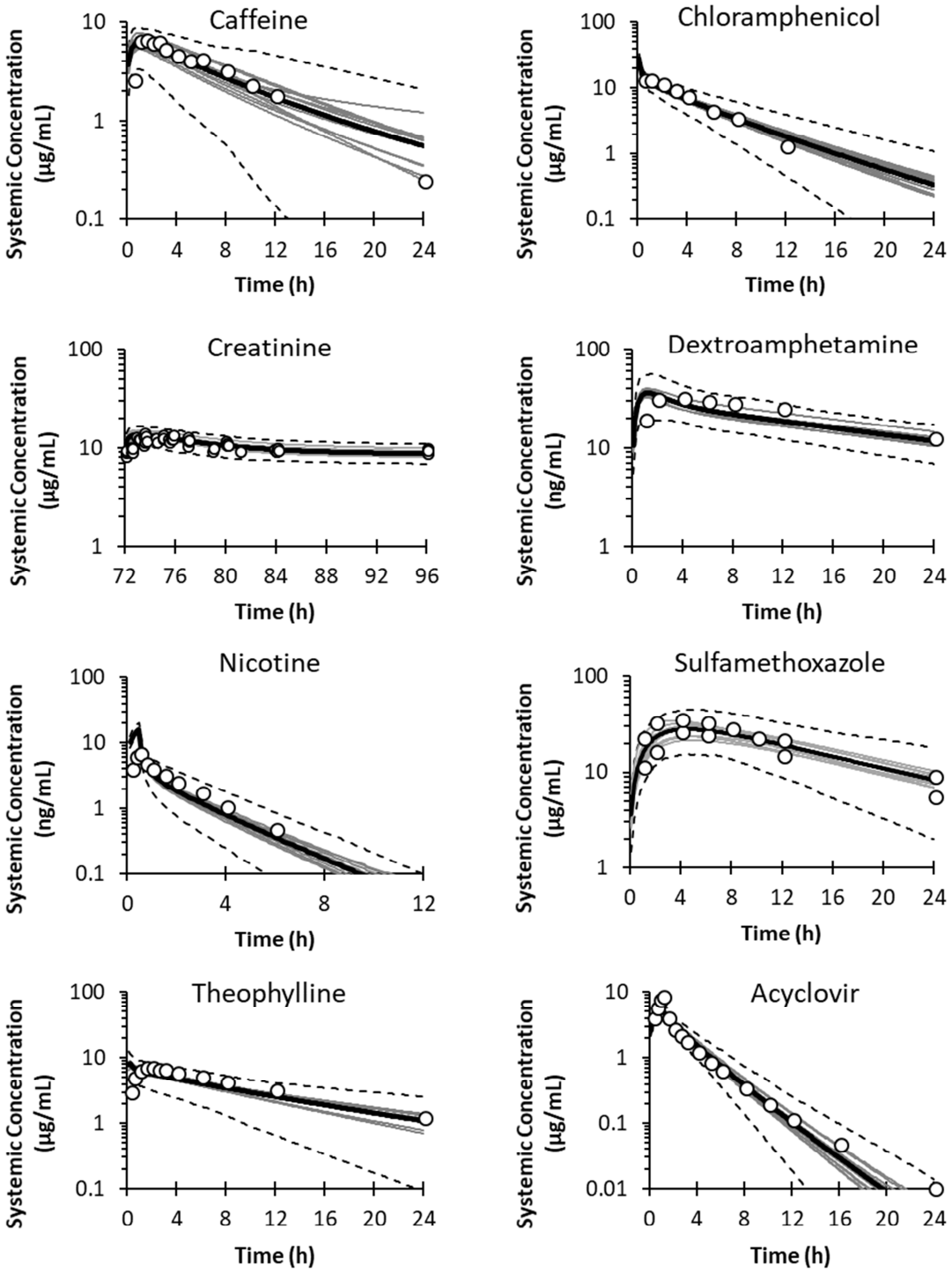

Figure S-4 Representative simulated plasma concentration-time profiles using initial PBPK models, without mechanistic prediction of CL_R. Initial PBPK models used a single input parameter derived from clinical data for CL_R (i.e. MechKiM was not activated). Bold black lines and dashed lines represent mean and 5th-95th percentile of 10 trials, respectively. Symbols indicate observed data.

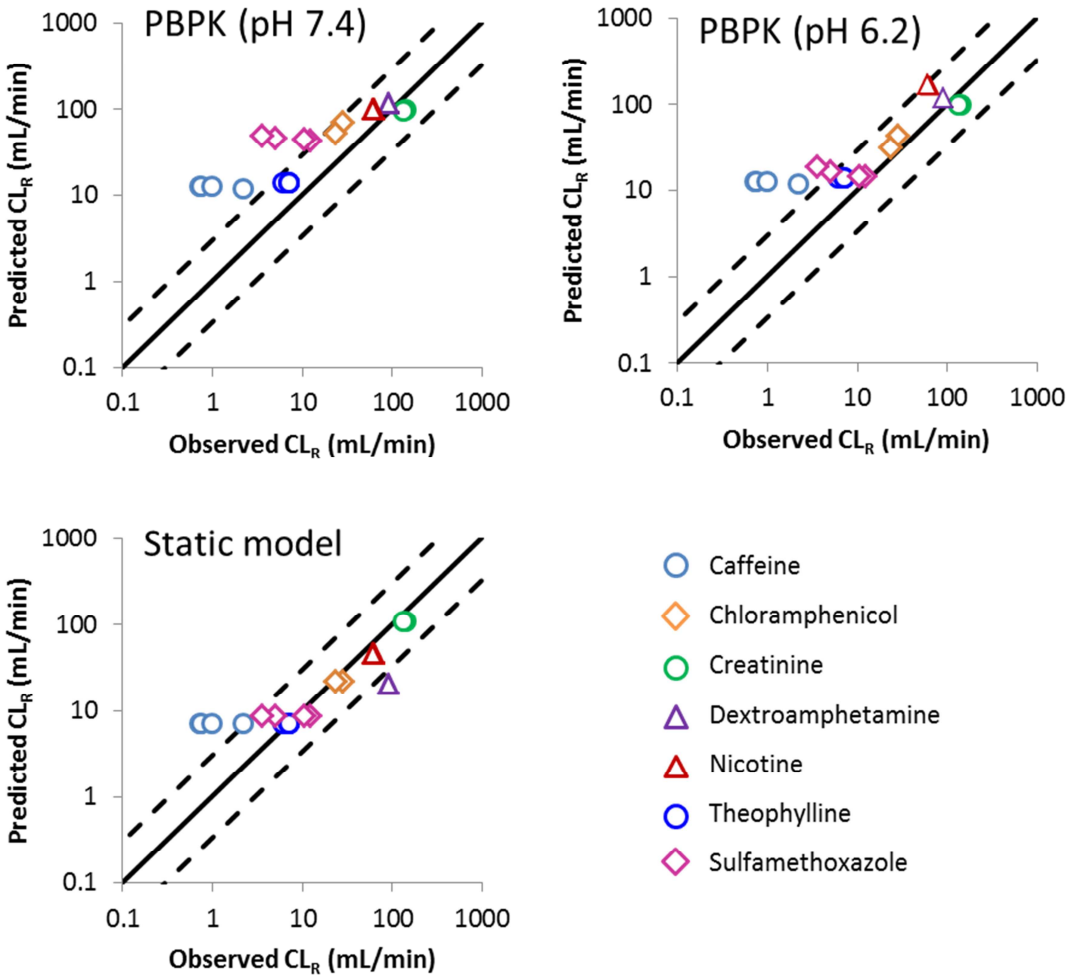

Figure S-5 Comparison between observed data and predicted CL_R by the PBPK model with MechKiM at urine pH of 7.4 and 6.2 or the static model.
Solid and dashed lines represent line of unity and 3-fold error, respectively. Each symbol represents the observed CL_R from a different study.

Table S-14 Predictability of renal clearance using IVIVE-prediction with mechanistic kidney model at normal condition.
For simulation using PBPK, urine/tubular pH at normal condition were assumed to be either 7.4 (Simcyp default value) or 6.2 (Rose et al).

Compounds	Dose Information	Number of subjects	Observed CL_R (mL/min)	Predicted CL_R (mL/min) *			Pred/Obs			Reference
				PBPK pH 7.4	PBPK pH 6.2	Static	PBPK pH 7.4	PBPK pH 6.2	Static	
Caffeine	50 mg Oral SD	5	2.17 ± 3.90	12.3 (7.3-20.8)	12.3 (7.3-20.8)	7.35	5.7 (3.4-9.6)	5.7 (3.4-9.6)	3.4	Newton (1981) (53)
	300 mg Oral SD	6	0.71 ± 0.24	13.1 (7.2-21.7)	13.1 (7.2-21.7)	7.35	18.5 (10.1-30.6)	18.5 (10.1-30.6)	10.3	Newton (1981) (53)
	500 mg Oral SD	6	0.74 ± 0.50	13.1 (7.2-21.7)	13.1 (7.2-21.7)	7.35	17.7 (9.7-29.3)	17.7 (9.7-29.3)	9.9	Newton (1981) (53).
	750 mg Oral SD	6	0.96 ± 0.30	13.1 (7.2-21.7)	13.1 (7.2-21.7)	7.35	13.6 (7.5-22.6)	13.6 (7.5-22.6)	7.7	Newton (1981) (53)
Chloramphenicol	CAPS 502-1324 mg IV SD	8	28.2 ± 25.8	70.3 (44.6-101.3)	44.4 (20.3-77.9)	22.4	2.5 (1.6-3.6)	1.6 (0.7-2.8)	0.80	Burke (1982) (8)
	CAPS 100 mg/kg/day IV infusion	1	23.1	53.7 (41.7-61.2)	32.0 (21.1-41.2)	22.4	2.3 (1.8-2.6)	1.4 (0.9-1.8)	1.0	Nahata (1981) (54)
Creatinine	Baseline (18.72 mg/kg/day)	6	139 ± 32	99.9 (76-133)	101 (77-134)	113	0.7 (0.5-1)	0.7 (0.6-1.0)	0.81	Mayersohn (1983) (55)
	Cooked meat (340 mg) Oral SD	6	132 ± 21	99.2 (76-132)	100 (76-133)	113	0.8 (0.6-1)	0.8 (0.6-1.0)	0.85	Mayersohn (1983) (55)
Dextroamphetamine	8.7 mg Oral SD	2	90 ± 67	118 (85-163)	120 (87-165)	21.2	1.3 (0.9-1.8)	1.3 (1.0-1.8)	0.24	Beckett (1969) (24)
Nicotine	0.028 mg/kg IV infusion for 10 min SD	20	63 ± 55	101 (62-154)	167 (124-227)	47.5	1.6 (1.0-2.4)	2.7 (2.0-3.6)	0.75	Molander (2001) (23)
	0.015 mg/kg IV infusion for 30 min SD	23	60 ± 49	100 (60-152)	168 (116-232)	47.5	1.7 (1.0-2.5)	2.8 (1.9-3.9)	0.79	Zevin (1997) (56)
Sulfamethoxazole	1000 mg IV infusion for 60 min SD	6	5.0	47.1 (30.9-70.7)	16.8 (6.2-39.6)	8.83	9.4 (6.2-14.1)	3.4 (1.2-7.9)	1.8	Mannisto (1982) (22)
	10 mg/kg IV infusion for 60 min SD	8	3.51 ± 1.52	50.1 (35.9-82.6)	18.9 (7.2-42.1)	8.83	14.3 (10.2-23.5)	5.4 (2.1-12)	2.5	Hutabarat (1991) (41)

	2000 mg Oral SD	16	12.3 ± 4.5	44.1 (30.9-59.6)	14.5 (5.9-26.4)	8.83	3.6 (2.5-4.8)	1.2 (0.5-2.1)	0.72	Kaplan (1973) (57)
	2000 mg Oral SD	8	10.5 ± 4.1	44.8 (30.7-64.6)	14.6 (6.2-28.9)	8.83	4.3 (2.9-6.2)	1.4 (0.6-2.8)	0.84	Kaplan (1973) (57)
Theophylline	125 mg Oral SD	8	5.89	14.3 (6.5-27)	13.5 (6.1-25.5)	7.34	2.4 (1.1-4.6)	2.3 (1-4.3)	1.2	Rovei (1982) (58)
	250 mg Oral SD	8	6.92	14.3 (6.5-27)	13.5 (6.1-25.5)	7.34	2.1 (0.9-3.9)	2.0 (0.9-3.7)	1.1	Rovei (1982) (58)
	375 mg Oral SD	8	6.92	14.3 (6.5-27)	13.5 (6.1-25.5)	7.34	2.1 (0.9-3.9)	2.0 (0.9-3.7)	1.1	Rovei (1982) (58)
	500 mg Oral SD	8	7.03	14.3 (6.5-27)	13.5 (6.1-25.5)	7.34	2.0 (0.9-3.8)	1.9 (0.9-3.6)	1.0	Rovei (1982) (58)

* Mean of 10 trials (5^{th} – 95^{th} percentile) for PBPK simulation
CAPS, chloramphenicol succinate.

Table S-15 Predictability of fraction reabsorbed using IVIVE-prediction with mechanistic kidney model at normal condition.
For simulation using PBPK, urine/tubular pH at normal condition were assumed to be either 7.4 (Simcyp default value) and 6.2 (Rose et al).

Compounds	Reference	Dose Information	Number of subjects	Observed CL_R (mL/min)	$CL_{R,filt}$ [a] (mL/min)	F_{reab} [b]			
						Observed	PBPK pH 7.4 [c]	PBPK pH 6.2 [c]	Static
Caffeine	Newton (1981) (53)	50 mg Oral SD	5	2.17 ± 3.90	81.6	0.97	0.85 (0.91, 0.75)	0.85 (0.91, 0.75)	0.91
	Newton (1981) (53)	300 mg Oral SD	6	0.71 ± 0.24	81.6	0.99	0.84 (0.91, 0.73)	0.84 (0.91, 0.73)	0.91
	Newton (1981) (53).	500 mg Oral SD	6	0.74 ± 0.50	81.6	0.99	0.84 (0.91, 0.73)	0.84 (0.91, 0.73)	0.91
	Newton (1981) (53)	750 mg Oral SD	6	0.96 ± 0.30	81.6	0.99	0.84 (0.91, 0.73)	0.84 (0.91, 0.73)	0.91
Chloramphenicol	Burke (1982) (8)	CAPS 502-1324 mg IV SD	8	28.2 ± 25.8	56.3	0.50	-0.25 (0.21, -0.8)	0.21 (0.64, -0.38)	0.60
	Nahata (1981) (54)	CAPS 100 mg/kg/day IV infusion	1	23.1	56.3	0.59	0.05 (0.26, -0.09)	0.43 (0.63, 0.27)	0.60
Creatinine	Mayersohn (1983) (55)	Baseline (18.72 mg/kg/day)	6	139 ± 32	120	-0.16	0.17 (0.37, -0.11)	0.16 (0.36, -0.12)	0.06
	Mayersohn (1983) (55)	Cooked meat (340 mg) Oral SD	6	132 ± 21	120	-0.10	0.17 (0.37, -0.10)	0.17 (0.37, -0.11)	0.06
Dextroamphetamine	Beckett (1969) (24)	8.7 mg Oral SD	2	90 ± 67	97.2	0.07	-0.21 (0.13, -0.68)	-0.23 (0.10, -0.7)	0.78
Nicotine	Molander (2001) (23)	0.028 mg/kg IV infusion for 10 min SD	20	63 ± 55	114	0.45	0.11 (0.46, -0.35)	-0.46 (-0.09, -0.99)	0.58
	Zevin (1997) (56)	0.015 mg/kg IV infusion for 30 min SD	23	60 ± 49	114	0.47	0.12 (0.47, -0.33)	-0.47 (-0.02, -1.03)	0.58
Sulfamethoxazole	Mannisto (1982) (22)	1000 mg IV infusion for 60 min SD	6	5.0	60.0	0.92	0.22 (0.49, -0.18)	0.72 (0.9, 0.34)	0.92
	Hutabarat (1991) (41)	10 mg/kg IV infusion for 60 min SD	8	3.51 ± 1.52	60.0	0.94	0.17 (0.4, -0.38)	0.69 (0.88, 0.3)	0.94
	Kaplan (1973) (57)	2000 mg Oral SD	16	12.3 ± 4.5	60.0	0.80	0.27 (0.49, 0.01)	0.76 (0.9, 0.56)	0.80

	Kaplan (1973) (57)	2000 mg Oral SD	8	10.5 ± 4.1	60.0	0.83	0.25 (0.49, -0.08)	0.76 (0.9, 0.52)	0.83
Theophylline	Rovei (1982) (58)	125 mg Oral SD	8	5.89	42.0	0.86	0.66 (0.85, 0.36)	0.68 (0.85, 0.39)	0.83
	Rovei (1982) (58)	250 mg Oral SD	8	6.92	42.0	0.84	0.66 (0.85, 0.36)	0.68 (0.85, 0.39)	0.83
	Rovei (1982) (58)	375 mg Oral SD	8	6.92	42.0	0.84	0.66 (0.85, 0.36)	0.68 (0.85, 0.39)	0.83
	Rovei (1982) (58)	500 mg Oral SD	8	7.03	42.0	0.83	0.66 (0.85, 0.36)	0.68 (0.85, 0.39)	0.83
Acyclovir	Soul-Lawton (1995) (30)	350 mg, 1h infusion	12	283 ± 103	102	-1.79	-1.59 (-0.36, -3.16)	-1.59 (-0.36, -3.16)	0.02
	Brigden (1981) (31)	50 mg IV bolus	6	185 ± 37	102	-0.82	-1.52 (-0.31, -3.88)	-1.52 (-0.31, -3.88)	0.02
	Brigden (1981) (31)	50 mg IV 1 h infusion	2	249	102	-1.45	-1.90 (-0.39, -4.41)	-1.90 (-0.39, -4.41)	0.02
	Brigden (1981) (31)	50 mg IV 10 min infusion	2	117	102	-0.15	-1.92 (-0.39, -4.48)	-1.92 (-0.39, -4.47)	0.02
	de Miranda (1981) (25)	0.5-2.5 mg/kg, IV infusion 1h	5	240 ± 77	102	-1.36	-1.52 (-0.22, -3.32)	-1.52 (-0.22, -3.32)	0.02
	Laskin (1982a) (32)	5 mg/kg, 1 h infusion	3	248 ± 46	102	-1.44	-1.62 (-0.21, -3.34)	-1.62 (-0.21, -3.34)	0.02
	Laskin (1982b) (33)	2.5 mg/kg, 1h infusion over 1h	3	158 ± 19	102	-0.56	-1.69 (-0.21, -3.32)	-1.69 (-0.21, -3.32)	0.02
	Laskin (1982b) (33)	5.0 mg/kg, 1h infusion over 1h	3	225 ± 100	102	-1.22	-1.69 (-0.21, -3.32)	-1.69 (-0.21, -3.32)	0.02
	Laskin (1982b) (33)	10 mg/kg, 1h infusion over 1h	4	238 ± 64	102	-1.34	-1.69 (-0.21, -3.57)	-1.69 (-0.21, -3.56)	0.02
	Laskin (1982b) (33)	15 mg/kg, 1h infusion over 1h	3	398 ± 67	102	-2.92	-1.69 (-0.21, -3.32)	-1.69 (-0.21, -3.32)	0.02

[a] $CL_{R,filt}$ (mL/min) = fu,plasma × GFR (120 mL/min).
[b] Freab = 1 - CL_R / $CL_{R,filt}$ [c] Mean of 10 trials (5^{th} – 95^{th} percentile) for PBPK simulation
CAPS, chloramphenicol succinate.

References

1. Snoeck E, Van Peer A, Sack M, Horton M, Mannens G, Woestenborghs R, et al. Influence of age, renal and liver impairment on the pharmacokinetics of risperidone in man. Psychopharmacology. 1995;122(3):223-9.

2. Martindale WH. The Extra Pharmacopoeia. 29th ed. London: The Pharmaceutical Press; 1989. 186 p.

3. Tóth B, Krajcsi P, Magnan R. Membrane transporters and transporter substrates as biomarkers for drug pharmacokinetics, pharmacodynamics, and toxicity/adverse events. In: Gupta. RC, editor. Biomarkers in Toxicology. 1st ed: Academic Press; 2014. p. 947-63.

4. Koup JR, Lau AH, Brodsky B, Slaughter RL. Chloramphenicol pharmacokinetics in hospitalized patients. Antimicrob Agents Chemother. 1979;15(5):651-7.

5. Matsson P, Bergstrom CA, Nagahara N, Tavelin S, Norinder U, Artursson P. Exploring the role of different drug transport routes in permeability screening. J Med Chem. 2005;48(2):604-13.

6. Karlsson J, Ungell A, Grasjo J, Artursson P. Paracellular drug transport across intestinal epithelia: influence of charge and induced water flux. Eur J Pharm Sci. 1999;9(1):47-56.

7. Tavelin S, Taipalensuu J, Soderberg L, Morrison R, Chong S, Artursson P. Prediction of the oral absorption of low-permeability drugs using small intestine-like 2/4/A1 cell monolayers. Pharm Res. 2003;20(3):397-405.

8. Burke JT, Wargin WA, Sherertz RJ, Sanders KL, Blum MR, Sarubbi FA. Pharmacokinetics of intravenous chloramphenicol sodium succinate in adult patients with normal renal and hepatic function. J Pharmacokinet Biopharm. 1982;10(6):601-14.

9. Valentin J. Basic anatomical and physiological data for use in radiological protection: reference values: ICRP Publication 89. Ann ICRP. 2002;32(3):1-277.

10. Perrin DD. Dissociation constants of organic bases in aqueous solution. London: Butterworths; 1965.

11. Barlow RB, Hamilton JT. Effects of ph on the activity of nicotine and nicotine monomethiodide on the rat diaphragm preparation. Br J Pharmacol Chemother. 1962;18(3):543-9.

12. Chen H, Gao B, Li H, Ma LQ. Effects of pH and ionic strength on sulfamethoxazole and ciprofloxacin transport in saturated porous media. J Contam Hydrol. 2011;126(1-2):29-36.

13. Eatman FB, Maggio AC, Pocelinko R, Boxenbaum HG, Geitner KA, Glover W, et al. Blood and salivary concentrations of sulfamethoxazole and trimethoprim in man. J Pharmacokinet Biopharm. 1977;5(6):615-24.

14. Franksson G, Anggard E. The plasma protein binding of amphetamine, catecholamines and related compounds. Acta Pharmacol Toxicol (Copenh). 1970;28(3):209-14.

15. Baggot JD, Davis LE, Neff CA. Extent of plasma protein binding of amphetamine in different species. Biochem Pharmacol. 1972;21(13):1813-6.

16. Benowitz NL, Jacob P, 3rd, Jones RT, Rosenberg J. Interindividual variability in the metabolism and cardiovascular effects of nicotine in man. J Pharmacol Exp Ther. 1982;221(2):368-72.

17. Scotcher D, Jones C, Rostami-Hodjegan A, Galetin A. Novel minimal physiologically-based model for the prediction of passive tubular reabsorption and renal excretion clearance. Eur J Pharm Sci. 2016;94:59-71.

18. Welling PG, Craig WA, Amidon GL, Kunin CM. Pharmacokinetics of trimethoprim and sulfamethoxazole in normal subjects and in patients with renal failure. J Infect Dis. 1973;128:Suppl:556-66 p.

19. Watanalumlerd P, Christensen JM, Ayres JW. Pharmacokinetic modeling and simulation of gastrointestinal transit effects on plasma concentrations of drugs from mixed immediate-release and enteric-coated pellet formulations. Pharm Dev Technol. 2007;12(2):193-202.

20. Skolnik S, Lin X, Wang J, Chen XH, He T, Zhang B. Towards prediction of in vivo intestinal absorption using a 96-well Caco-2 assay. J Pharm Sci. 2010;99(7):3246-65.

21. Benowitz NL, Jacob P, 3rd. Nicotine and cotinine elimination pharmacokinetics in smokers and nonsmokers. Clin Pharmacol Ther. 1993;53(3):316-23.

22. Mannisto PT, Mantyla R, Mattila J, Nykanen S, Lamminsivu U. Comparison of pharmacokinetics of sulphadiazine and sulphamethoxazole after intravenous infusion. J Antimicrob Chemother. 1982;9(6):461-70.

23. Molander L, Hansson A, Lunell E. Pharmacokinetics of nicotine in healthy elderly people. Clin Pharmacol Ther. 2001;69(1):57-65.

24. Beckett AH, Salmon JA, Mitchard M. The relation between blood levels and urinary excretion of amphetamine under controlled acidic and under fluctuating urinary pH values using [14C] amphetamine. J Pharm Pharmacol. 1969;21(4):251-8.

25. de Miranda P, Good SS, Laskin OL, Krasny HC, Connor JD, Lietman PS. Disposition of intravenous radioactive acyclovir. Clin Pharmacol Ther. 1981;30(5):662-72.

26. Blum MR, Liao SH, de Miranda P. Overview of acyclovir pharmacokinetic disposition in adults and children. Am J Med. 1982;73(1A):186-92.

27. Yee S. In vitro permeability across Caco-2 cells (colonic) can predict in vivo (small intestinal) absorption in man--fact or myth. Pharm Res. 1997;14(6):763-6.

28. Yazdanian M, Glynn SL, Wright JL, Hawi A. Correlating partitioning and caco-2 cell permeability of structurally diverse small molecular weight compounds. Pharm Res. 1998;15(9):1490-4.

29. Parr A, Hidalgo IJ, Bode C, Brown W, Yazdanian M, Gonzalez MA, et al. The Effect of Excipients on the Permeability of BCS Class III Compounds and Implications for Biowaivers. Pharm Res. 2016;33(1):167-76.

30. Soul-Lawton J, Seaber E, On N, Wootton R, Rolan P, Posner J. Absolute bioavailability and metabolic disposition of valaciclovir, the L-valyl ester of acyclovir, following oral administration to humans. Antimicrob Agents Chemother. 1995;39(12):2759-64.

31. Brigden D, Bye A, Fowle AS, Rogers H. Human pharmacokinetics of acyclovir (an antiviral agent) following rapid intravenous injection. J Antimicrob Chemother. 1981;7(4):399-404.

32. Laskin OL, de Miranda P, King DH, Page DA, Longstreth JA, Rocco L, et al. Effects of probenecid on the pharmacokinetics and elimination of acyclovir in humans. Antimicrob Agents Chemother. 1982;21(5):804-7.

33. Laskin OL, Longstreth JA, Saral R, de Miranda P, Keeney R, Lietman PS. Pharmacokinetics and tolerance of acyclovir, a new anti-herpesvirus agent, in humans. Antimicrob Agents Chemother. 1982;21(3):393-8.

34. Birkett DJ, Miners JO. Caffeine renal clearance and urine caffeine concentrations during steady state dosing. Implications for monitoring caffeine intake during sports events. Br J Clin Pharmacol. 1991;31(4):405-8.

35. Blanchard J, Sawers SJ. Relationship between urine flow rate and renal clearance of caffeine in man. J Clin Pharmacol. 1983;23(4):134-8.

36. Tang-Liu DD, Tozer TN, Riegelman S. Dependence of renal clearance on urine flow: a mathematical model and its application. J Pharm Sci. 1983;72(2):154-8.

37. Feyerabend C, Russell MAH. Effect of urinary pH and nicotine excretion rate on plasma nicotine during cigarette smoking and chewing nicotine gum. Br J Clin Pharmacol. 1978;5(4):293-7.

38. Benowitz NL, Jacob P, 3rd. Nicotine renal excretion rate influences nicotine intake during cigarette smoking. J Pharmacol Exp Ther. 1985;234(1):153-5.

39. Vree TB, Hekster YA, Baars AM, Damsma JE, van der Kleijn E. Pharmacokinetics of sulphamethoxazole in man: effects of urinary pH and urine flow on metabolism and renal excretion of sulphamethoxazole and its metabolite N4-acetylsulphamethoxazole. Clin Pharmacokinet. 1978;3(4):319-29.

40. Sharpstone P. The renal handling of trimethoprim and sulphamethoxazole in man. Postgrad Med J. 1969;45(Suppl):38-42.

41. Hutabarat RM, Unadkat JD, Sahajwalla C, McNamara S, Ramsey B, Smith AL. Disposition of drugs in cystic fibrosis. I. Sulfamethoxazole and trimethoprim. Clin Pharmacol Ther. 1991;49(4):402-9.

42. Tang-Liu DD, Tozer TN, Riegelman S. Urine flow-dependence of theophylline renal clearance in man. J Pharmacokinet Biopharm. 1982;10(4):351-64.

43. Guyton AC, Hall J. Guyton and Hall Textbook of Medical Physiology. 11 ed: Elsevier Saunders; 2005.

44. Matsukura S, Sakamoto N, Takahashi K, Matsuyama H, Muranaka H. Effect of pH and urine flow on urinary nicotine excretion after smoking cigarettes. Clin Pharmacol Ther. 1979;25(5 Pt 1):549-54.

45. Branch RA, Read PR, Levine D, Elst EV, Shelton J, Rupp W, et al. Furosemide and bumetanide: a study of responses in normal English and German subjects. Clin Pharmacol Ther. 1976;19(5 Pt 1):538-45.

46. Bloomfield SS, Tetreault L. A Pharmacology Teaching Exercise in Drug Evaluation: A Comparison of the Diuretic Efficacy of Clorexolone, Hydrochlorothiazide and a Placebo in Normal Subjects. Can Med Assoc J. 1965;92:662-5.

47. Gheorghiade M, Niazi I, Ouyang J, Czerwiec F, Kambayashi J, Zampino M, et al. Vasopressin V2-receptor blockade with tolvaptan in patients with chronic heart failure: results from a double-blind, randomized trial. Circulation. 2003;107(21):2690-6.

48. Goldsmith SR, Gilbertson DT, Mackedanz SA, Swan SK. Renal effects of conivaptan, furosemide, and the combination in patients with chronic heart failure. J Card Fail. 2011;17(12):982-9.

49. Nussberger J, Mooser V, Maridor G, Juillerat L, Waeber B, Brunner HR. Caffeine-induced diuresis and atrial natriuretic peptides. J Cardiovasc Pharmacol. 1990;15(5):685-91.

50. Wemple RD, Lamb DR, McKeever KH. Caffeine vs caffeine-free sports drinks: effects on urine production at rest and during prolonged exercise. Int J Sports Med. 1997;18(1):40-6.

51. Nielsen OE. Comparative studies of the diuretics acetazolamide, aminometradine, chlorothiazide and theophylline. Acta Pharmacol Toxicol (Copenh). 1961;18:23-37.

52. Perazella MA. Renal vulnerability to drug toxicity. Clin J Am Soc Nephrol. 2009;4(7):1275-83.

53. Newton R, Broughton L, Lind M, Morrison P, Rogers H, Bradbrook I. Plasma and salivary pharmacokinetics of caffeine in man. Eur J Clin Pharmacol. 1981;21(1):45-52.

54. Nahata MC, Powell DA. Bioavailability and clearance of chloramphenicol after intravenous chloramphenicol succinate. Clin Pharmacol Ther. 1981;30(3):368-72.

55. Mayersohn M, Conrad KA, Achari R. The influence of a cooked meat meal on creatinine plasma concentration and creatinine clearance. Br J Clin Pharmacol. 1983;15(2):227-30.

56. Zevin S, Jacob P, 3rd, Benowitz N. Cotinine effects on nicotine metabolism. Clin Pharmacol Ther. 1997;61(6):649-54.

57. Kaplan SA, Weinfeld RE, Abruzzo CW, McFaden K, Jack ML, Weissman L. Pharmacokinetic profile of trimethoprim-sulfamethoxazole in man. J Infect Dis. 1973;128(Supplement 3):Suppl:547-55 p.

58. Rovei V, Chanoine F, Strolin Benedetti M. Pharmacokinetics of theophylline: a dose-range study. Br J Clin Pharmacol. 1982;14(6):769-78.